Fully Dynamic Rate Theory (FDRT) Simulation of Radiation Induced Swelling of Metals

N. Ghoniem and G.L. Kulcinski

October 1976

UWFDM-180

FUSION TECHNOLOGY INSTITUTE

UNIVERSITY OF WISCONSIN

MADISON WISCONSIN

Fully Dynamic Rate Theory (FDRT) Simulation of Radiation Induced Swelling of Metals

N. Ghoniem and G.L. Kulcinski

Fusion Technology Institute
University of Wisconsin
1500 Engineering Drive
Madison, WI 53706

http://fti.neep.wisc.edu

October 1976

UWFDM-180

"LEGAL NOTICE"

"This work was prepared by the University of Wisconsin as an account of work sponsored by the Electric Power Research Institute, Inc. ("EPRI"). Neither EPRI, members of EPRI, the University of Wisconsin, nor any person acting on behalf of either:

"a. Makes any warranty or representation, express or implied, with respect to the accuracy, completeness, or usefulness of the information contained in this report, or that the use of any information, apparatus, method, or process disclosed in this report may not infringe privately owned rights; or

"b. Assumes any liabilities with respect to the use of, or for damages resulting from the use of, any information, apparatus, method or process disclosed in this report."

Fully Dynamic Rate Theory (FDRT) Simulation of Radiation Induced Swelling of Metals

N. Ghoniem

G. Kulcinski

November 1976

UWFDM-180

Fusion Technology Program
Nuclear Engineering Department
University of Wisconsin
Madison, Wisconsin 53706

Abstract

A quantitative theoretical understanding of the void growth phenomenon is vital to the experimental metal swelling programs. This paper describes a Time Dependent Rate Theory Model of void growth and it is correlated to experimental results. It is shown that reasonable agreement between theoretical and experimental swelling data can be obtained for 316 stainless steel under steady state electron and ion irradiations. This model is then applied to pulsed irradiation to study the effects of annealing between pulses on the reduction of swelling. It is concluded that there exists a temperature dependent critical time in between pulses, t_p^{crit}, such that if the time between pulses is greater than t_p^{crit} voids shrink and at $t < t_p^{crit}$ voids will grow.

TABLE OF CONTENTS

	Page
I. Introduction	1
II. Steady State Theoretical Models of Void Growth	3
II. 1. The Cellular Model	5
II. 2. The Rate Theory Model	6
III. Fully Dynamic Rate Theory (FDRT)	7
IV. Numerical Aspects and Solution of the FDRT	15
V. FDRT Applied to Time Independent Irradiations	20
V. 1. 1 MeV Electron Irradiation of M316 S.S.	20
V. 2. 22 MeV C^{++} Ion Bombardment of M316 S.S.	
VI. FDRT Applied to Pulsed Irradiations	26
VI. 1. Laser Fusion Pulsed System	26
VI. 2. Analysis and Results	27
VII. Concluding Remarks	36

Fully Dynamic Rate Theory (FDRT) Simulation of Radiation Induced Swelling of Metals

N. M. GHONIEM and G. L. KULCINSKI

I. Introduction

The steady-state rate theory model for void induced swelling was originally developed by Harkness and Li (1969,1971)[1,2,3] and by Wiedersich (1972)[4] and has been expanded by Brailsford and Bullough (1972,1973).[5,6] The object of this work is to extend the previous work to include dynamic effects. We first describe the time-dependent rate theory model in its general case, and then develop an analysis applicable to specific material and irradiation conditions. The procedure in this paper is to preserve the physical picture, as much as possible, away from mathematical difficulties which are explained in more detail elsewhere.[11]

The idea in a rate theory model is to replace all the discrete sinks in the solid, including the voids, by equivalent homogeneous distributions of sinks in a continuum. In this continuum, the various sinks are given different strengths to insure that the flux of defects will be as close as possible to the flux at the actual (geometrical) sinks in the real solid. Replacing the discrete and actual distributions of sinks by an equivalent and idealized continuous distribution will have the obvious advantage of space independence of the problems and should be especially applicable to heavily damaged structures. With such boundary conditions the vacancy and interstitial concentrations, and the governing equations for these concentrations now reduce to a simpler pair of time dependent equations.

The simultaneous equations for C_i and C_v, the time dependent interstitial and vacancy concentrations (far from sources and sinks), have the form:

{production rate}-{sink removal rate}-{recombination rate}={rate of change of defect concentration}.

Previous treatments of the rate theory applied to metal swelling under irradiation also assumed either a steady state situation for all material parameters during irradiation, or a quasi-steady state situation. Cellular models and early homogeneous rate theories also assumed the existence of a steady state point defect concentration as well as constant sink strengths.

In this effort, we try to study the time behavior of relevant materials parameters. Experimental and theoretical investigations have revealed many facts about the time behavior of different microstructure parameters, for example, it is known that the nucleation of voids and dislocation loops is much faster than their subsequent growth. If one would use the expression of a "time constant" to describe the time behavior of a certain process, then the nucleation time constant (1/time for process to occur) is much larger than the growth time constant. Also the interstitial concentration time constant for any process is always larger than the similar vacancy concentration time constant. Both vacancy and interstitial time constants are larger than the void or interstitital dislocation loop nucleation time constants.

During irradiation, there is a time period during which the defect removal rate to sinks and the recombination rates change rapidly. This happens at the start of irradiation when the materials parameters are driven by the rapid changes of Frenkel pair concentrations with time. An important consequence of this situation is that there will be a different behavior of all the physical parameters that describe the microstructure of the material under irradiation. Among these quantities of

interest are the nucleation rates, the size distribution of embryoes and the forward and backward reactions that lead to microstructure evolution. Examples of the latter process are the growth kinetics of voids and dislocation loops. This paper will only consider the growth of these defects and subsequent work will treat the nucleation phenomena.

II. Steady-State Theoretical Models of Void Growth

Voids grow ultimately because edge dislocations have a stronger attraction for interstitials than for vacancies. While it is true that vacancies are certainly attracted to dislocations, the larger distortion field associated with an interstitial results in a stronger attraction (particularly to the dilated region) and thus a preferential drift. The dislocations thus act as sinks for both vacancies and interstitials but are more effective for interstitials and the relative strength of this bias for interstitials can be estimated from our basic knowledge of point defect-dislocation interactions. Suitable dislocations are always present during the irradiation, some because they were present before the irradiation and others as a result of interstitial and vacancy clustering during the irradiation. Irradiation produces vacancies and interstitials at an identical rate and since the interstitials are much more mobile than the vacancies they will very soon begin to form interstitial clusters which quickly transform to interstitial dislocation loops which are usually pure edge in character. The growth of these loops will then be

facilitated by the preferential drift of more interstitials. This slight preferential loss of interstitials to the dislocations means that the net point defect flux into any other neutral sink, such as the small gas bubble (void embryo), will be vacancy in character and thus void nuclei will grow. Void growth thus requires at least one other sink type in addition to the void nuclei and that additional sink must have a preferential bias for interstitials. The steady state concentrations of vacancies and interstitials are achieved as a result of loss of such defects at sinks and by mutual recombination.

In addition to forming voids,some vacancies will form small vacancy loops in the center of the displacement spikes.[23] Such loops will also preferentially attract interstitials and therefore their growth should be inhibited. However, the kinetics of void growth may be influenced by the transient presence of such vacancy loops because they tie up vacancies that normally would have contributed to more swelling.

In the last few years,several theories of the void growth process have been developed with the principle object of correlating and explaining the available swelling data from reactors, accelerators and the high voltage electron microscopes. It is hoped that such theories, when based on sound physical principles and correlated with data, may be used to confidently predict the swelling behaviour of different materials subjected to neutron doses greater than those achievable in the present testing facilities. Such extrapolations will assist designers in the choice of materials for future reactor components.

As stated previously, all the current theories of void growth are based on the fundamental hypothesis (which is supported by a wide range of metallurgical experience) that the interstitials are preferentially attracted

to the existing dislocations compared with the vacancies. Such theories may be divided into two classes:

II. 1. The Cellular Model

In this model the body containing N_v voids per unit volume is divided into spherical cells, each initial of radius R_o where

$$R_o = 0.68\ N_v^{-1/3} \qquad (1)$$

and each with a spherical void, of radius $r_v(0)$ at its center. This approach has been developed in a series of papers by Bullough and Perrin (1971, 1972)[7,8] and by Forman (1971)[9]. The other sinks in the body, be they biased (dislocations) or neutral (precipitates), are continuously distributed throughout the body. The subsequent swelling may then be studied by following the growth of one such void when diffusion processes are permitted in the cellular region around it.

The disadvantage with this model is that the governing diffusion equations for the steady-state interstitial and vacancy concentrations are second order non-linear simultaneous equations; the non-linearity arises from the recombination terms which are proportional to the product of the interstitial and vacancy concentration and also couple the equations.

A more convenient theory is the rate theory approach which is discussed below.

II. 2. The Rate Theory Model

The simultaneous equations for C_i and C_v, the steady-state interstitial and vacancy concentrations, have the form

$$P - D_i C_i k_i^2 - \alpha C_i C_v = 0 \tag{2}$$

$$P' - D_v C_v k_v^2 - \alpha C_i C_v = 0 \tag{3}$$

where D_i, D_v are respectively the interstitial and vacancy diffusion coefficients, α is the recombination coefficient, P is the point defect generation rate* and P' is the enhanced defect generation rate for the vacancies, incorporating their thermal emission from the dislocations and neutral sinks (voids). The parameters k_i and k_v have been deduced by carefully calculating the effective sink strengths in the continuum in relation to their strengths in the real body. In fact, k_i^{-1} and k_v^{-1} represent the mean free path of an interstitial or vacancy respectively to a sink.

The sink parameters have the explicit form[5]

$$k_i^2 = Z_i \rho_d + 4\pi r_v N_v + Y_i \, 4\pi r_p C_p \tag{4}$$

$$k_v^2 = Z_v \rho_d + 4\pi r_v N_v + Y_v \, 4\pi r_p C_p \tag{5}$$

where N_v is the concentration of voids of radius r_v and ρ_d is the total dislocation density,

$$\rho_d = \rho_d^L + \rho_d^o \, . \tag{6}$$

In this division of ρ_d, ρ_d^L is the irradiation produced dislocation density in the form of interstitial loops and ρ_d^o is the original (deformation produced) dislocation network density. The quantities

* generation rates are expressed as fraction per second

Z_i and Z_v define the percent preference that dislocations are assumed to have for interstitials. Finally, C_p is the concentration of coherent precipitate sinks of radius r_p. As the irradiation proceeds the quantities ρ_d^L and r_v will increase; the latter neutral sink radius can represent either a void growing from an embryonic gas bubble or a void growing on an incoherent precipitate. In either case the transient variation of r_v defines the required swelling kinetics. In contrast, the radius of any coherent sinks r_p will not change since it is assumed that such coherence precludes accumulation of point defects of either type. The net result of such sinks is an enhanced recombination rate and the failure to accumulate defects requires that such sinks automatically must generate an induced preference for interstitials (to compensate for the interstitial depletion at the dislocations). To achieve this, their strength is defined by the Y_i, Y_v parameters in Eqs. (4) and (5).

III. Fully dynamic Rate Theory (FDRT)

Bullough, Eyre and Krishan (BEK hereafter) extended the steady state rate theory (SSRT)[10] to include the formation of vacancy loops from displacement cascasdes. A quasi-steady state description of the Frenkel pair concentrations was used. The effort in this paper is an extension of the BEK rate theory, including the formation of vacancy loops in collision cascades, to allow for possible time-dependent applications of the theory. One of the main difficulties in this extension is the wide range of the "time constants" of this problem as shown later.

Now let $r_{v\ell}(0)$ be the average radius of the vacancy loops immediately following their athermal formation. To be consistent with

the content of defects in typical cascades,[23] $r_{v\ell}(0)$ will be taken to be 15 Angstroms. We also introduce the parameter ε, where, if P is the fractional Frenkel pair production rate, then εP is the fractional rate at which vacancies are removed from solution to form vacancy loops. To study the growth of voids, ε could be used as an adjustable parameter to account for the subtle distinction between electron irradiation (where $\varepsilon = 0$), heavy ion irradiation and neutron irradiation.

If b is the magnitude of the Burger's vector, the atomic volume is b^3 and $n_{v\ell}$ is the fractional concentration* of vacancy loops created per second, then:

The number of vacancies in a vacancy loop = $\pi\, r_{v\ell}^2 b/b^3$ (7)

and

$$n_{v\ell} = \frac{\varepsilon P b^2}{\pi\, r_{v\ell}^2(0)} \quad . \tag{8}$$

When a vacancy loop has formed, it will immediately act as an interstitial sink because of the dislocation character of its perimeter. It will then instantly be attacked by interstitials and consequently shrink. At high temperatures the loops will also shrink by thermal emission and this process will be greatly assisted by the high line tension of such small loops and by the stacking fault energy if the loops remain faulted. Thus, each loop will have a finite lifetime τ and the number of vacancy loops per unit volume, $N_{v\ell}$, present at any time t is given by the simple rate equation

$$\frac{dN_{v\ell}(t)}{dt} = \frac{n_{v\ell}}{b^3} - \frac{N_{v\ell}(t)}{\tau} \tag{9}$$

---

* Here fractional concentration refers to number of loops per atomic lattice site

where the first term on the righthand side is the loop generation rate and the second term represents the loss term due to shrinkage.

The lifetime, τ, of an individual loop is a function of time in the sense that it depends on the state of the overall sink distribution prevailing at its instant of creation. From a Taylor series expansion of $r_{v\ell}(t)$ we have

$$\tau = \tau(t) \simeq -\frac{r_{v\ell}(o)}{(dr_{ve}/dt)_{[r_{v\ell}(o)]}} \quad . \tag{10}$$

To calculate the shrinkage rate of vacancy loops, one has to explicitly write the rate equation for an individual vacancy loop

$$\frac{dr_{v\ell}(t)}{dt} = \frac{1}{b}\left\{Z_V D_V C_V(t) - Z_I D_I C_I(t) - Z_V D_V C_V^o \exp\left(\left[\frac{\gamma_{sf} + F_{el}(r_{v\ell})}{kT}\right]\right)\right. \tag{11}$$

Here, one defines:

Z_V = dislocation bias for vacancies, normally taken to be unity

Z_I = dislocation bias for interstitials, > 1.0

D_V = vacancy diffusion coefficient, cm^2/sec

D_I = interstitial diffusion coefficient, cm^2/sec

C_V^o = the thermal equilibrium concentration of vacancies (at./at.)

$C_V(t)$ = fractional vacancy concentration (at./at.)

k = Boltzmann's constant (ev/^oK)

T = temperature (^oK)

γ_{sf} = stacking fault energy (ev/cm^2)

and

$$F_{el} = \frac{\mu b^2}{(1-\nu)4\pi(r+b)} \ln\left(\frac{r+b}{b}\right) \tag{12}$$

is a bounded form (at $r = o$) for the elastic energy of a dislocation loop of radius r, and

μ = shear modulus (dynes/cm^2)

ν = Poisson's ratio.

The loop lifetime will then have the form

$$\tau(t) \tilde{=} r_{v\ell}(o)b/\{Z_I D_I C_I(t) + Z_V D_V C_V(t) \exp\left\{\left[\frac{\gamma_{sf} + F_{el}(r_{v\ell}(o))}{kT}\right] b^2\right\}$$

$$-Z_V D_V C_V(t)\} \tag{13}$$

The atomic (at/at) concentration of vacancies in vacancy loops

$$q_{V\ell} = \pi b r_{v\ell}^2 N_{v\ell} \cdot \tag{14}$$

Hence the rate equation for the fractional rate of change of vacancies in vacancy loops would then be:

$$\frac{dq_{v\ell}(t)}{dt} = \varepsilon P - \sqrt{4\pi q_{V\ell}(t) N_{v\ell}(t)/b}\,\{Z_I D_I C_I(t) - Z_V D_V C_V(t)$$

$$+ Z_V D_V C_V^o \quad \exp\left([\gamma_{sf} + F_{el}(r_{v\ell})]\, b^2/kT\right)\} \,. \tag{15}$$

The void radius rate of change is given by,

$$\frac{dr_V(t)}{dt} = \frac{1}{r_V(t}\left\{D_V C_V(t) - D_i C_i(t) - D_V C_V^o \exp\left[\left(\frac{2\gamma}{r_V(t)} - p_g\right)\frac{b^3}{kT}\right]\right\} \,, \tag{16}$$

here

r_V = void radius (cm)

γ = surface energy (eV/cm^2)

p_g = gas pressure inside the void (eV/cm^3)

$$p_g = \frac{3n_g kT}{4\pi(r_V^3 - 3b_V n_g/4\pi)} \tag{17}$$

n_g = the number of gas atoms within each void

b_V = Van der Waal's coefficient. $(\frac{cm^3}{atom})$

The percentage swelling is given by

$$S = \frac{4}{3}\pi r_V^3 N_V \times 100 \tag{18}$$

where N_V is the number of voids/cm^3.

For interstitial loops in the stress free case, the following rate equation would apply

$$\frac{dr_{i\ell}}{dt} = \frac{1}{b}\left[Z_I D_I C_I(t) - Z_V D_V C_V(t) + Z_V D_V C_V^o \times \right.$$

$$\left. \exp\left\{-\left[\gamma_{sf} + F_{el}(r_{i\ell})\right] b^2/kT\right\}\right] . \qquad (19)$$

Under pulsed irradiation conditions the point defect concentrations will never be in a steady state so it is now interesting to study the time for the point defects to reach a quasi-steady state equilibrium with the time varying sinks. The relative importance of recombination and loss to sinks can be determined by using a Fully Dynamic Rate Theory (FDRT) formulation. Let us now follow the different rate processes for point defects.

The two time-dependent rate equations for point defects are given by

$$P(t) - \lambda_I(t)C_I(t) - \alpha C_I(t)C_V(t) = \frac{dC_I(t)}{dt} \qquad (20)$$

and

$$P_e(t) + (1 - \epsilon)\, P(t) - \lambda_V(t)C_V(t) - \alpha C_I(t)C_V(t) = \frac{dC_V(t)}{dt} \quad . \qquad (21)$$

Now if we define

$P_R(t)$ = rate of recombination (at./at./sec.)

$P_{SI}(t)$ = rate of interstitial leakage to all sinks (at./at./sec.)

$P_{SV}(t)$ = rate of vacancy leakage to all sinks (at./at./sec.)

$P_e(t)$ = rate of vacancy emission from all sinks (at./at./sec.) and can be restated as

$$P_e(t) = P_e^V(t) + P_e^d(t) + P_e^{i\ell}(t) + P_e^{v\ell}(t) \tag{22}$$

where

$P_e^V(t)$ is the rate of thermal vacancy emission from voids,

$P_e^d(t)$ is the rate of thermal vacancy emission from edge dislocations,

$P_e^{i\ell}(t)$ is the rate of thermal vacancy emission from interstitial loops, and

$P_e^{v\ell}(t)$ is the rate of thermal vacancy emission from vacancy loops.

The various terms in Equation 22 are:

$$P_e^V(t) = 4\pi r_V(t) N_V C_V^o \exp\left[(2\gamma/r_V(t) - p_g)\, b^3/kT\right] \tag{23}$$

$$P_e^d(t) = Z_V \rho_d^o D_V C_V^o \tag{24}$$

$$P_e^{i\ell}(t) = Z_V \rho_d^{i\ell} D_V C_V^o \tag{25}$$

$$P_e^{v\ell}(t) = Z_V \rho_d^{v\ell} D_V C_V^o \,. \tag{26}$$

The interstitial loop dislocation density is given by

$$\rho_d^{i\ell}(t) = 2\pi r_{i\ell}(t) N_{i\ell} \tag{27}$$

and

$$\rho_d^{v\ell}(t) = 2\pi r_{v\ell}(t) N_{v\ell}(t) \tag{28}$$

is the vacancy loop dislocation density in cm/cm^3.

Now

$$P_R(t) = \alpha C_I(t) C_V(t) \tag{29}$$

where α is the recombination coefficient and given as

$$\alpha = g(\nu_I e^{-E_I^m/kT} + \nu_V e^{-E_V^m/kT}) \ . \tag{30}$$

In Equation 30, g is the combinatory number, ν_I is the interstitial frequency, ν_V is the vacancy frequency, E_I^m is the interstitial migration energy, and E_V^m is the vacancy migration energy.

$$P_{SI}(t) = \lambda_I(t) C_I(t) \tag{31}$$

$\lambda_I(t)$ is a time dependent total interstitial leakage time constant

$$\lambda_I(t) = \lambda_I^V(t) + \lambda_I^d(t) \tag{32}$$

and

$$\lambda_I^V(t) = 4\pi r_V(t) N_V D_I \tag{33}$$

is the interstitial leakage time constant for voids and (34)

$$\lambda_I^d(t) = Z_I D_I(\rho_d^o + \rho_d^{V\ell}(t) + \rho_d^{I\ell}(t)) \tag{35}$$

is the interstitial leakage time constant for dislocations. (36)

Also

$$P_{SV}(t) = \lambda_v(t)C_v(t)$$

$\lambda_v(t)$ is a time dependent total vacancy leakage time constant

$$\lambda_v(t) = \lambda_v^V(t) + \lambda_v^d(t) \tag{37}$$

where

$$\lambda_v^V(t) = 4\pi r_V(t)N_V D_V \tag{38}$$

is the vacancy leakage time constant for voids and

$$\lambda_v^d(t) = Z_V D_V(\rho_d^o + \rho_d^{V\ell}(t) + \rho_d^{I\ell}(t)) \tag{39}$$

is the vacancy leakage time constant for dislocations.

According to the previous definitions, Equations (20) and (21) for the time rate of change of Frenkel pairs could be written as:

$$\frac{dC_I(t)}{dt} = P(t) - P_{SI}(t) - P_R(t) \tag{40}$$

and

$$\frac{dC_V(t)}{dt} = P_v^e(t) + (1-\varepsilon)P(t) - P_{SV}(t) - P_R(t) \ . \tag{41}$$

IV. Numerical aspects and Solution of the FDRT:

Equations (11), (15), (16), (19), (20), and (21) represent six non-linear interdependent first order differential equations. In the

following we present the highlights of the calculational method used to solve this system. A computer code "TRANSWELL" has been developed to simulate TRANSIENT SWELLING irradiations. The details of the computations and a description of "TRANSWELL" is given elsewhere. (11)

One of the difficulties of solving time dependent materials problems is the "stiffness" of the resulting system of equations describing the phenomenon. Roughly speaking, an ordinary differential equation (ODE) system is called stiff if it involves both very rapidly changing terms and very slowly changing terms, all of a decaying nature. More precisely, we consider the eigen values λ_i of the N x N Jacobian matrix

$$J = \frac{\partial f}{\partial y} = \left(\frac{\partial f_i}{\partial y_j}\right)_{i,j=1}^{N},$$

and suppose that the λ_i all have negative real parts. The "time constants" of the problem are then $\tau_i = 1/|Re(\lambda_i)|$ and the local decaying nature of the solution is given by the exponentials e^{-t/τ_i}. If the N time constants τ_i are widely spread, and those terms with the smaller τ_i have already decayed to an insignificant level, while those with larger τ_i's have been hardly effected, then the system is stiff. Actually, some of the $R_e(\lambda_i)$ may be non-negative (meaning that some solution components are non-decaying), and the system would still be called stiff if some of the remaining negative $R_e(\lambda_i)$ have a relatively large magnitude. It should also be recognized that the property of stiffness is local; that is a problem may be stiff in some regions of t and not in others. Finally, a relative measure of the stiffness is the ratio (max τ_i/min τ_i).

The difficulty with stiff problems is that most conventional methods for solving ODE's require the incremented values of time commensurate with min τ_i, while the size $|T-t_o|$ of the problem range is commensurate with max τ_i. As a result, the problem cannot be run to completion in a reasonable number of steps.

The above problem can be addressed by using a numerical method developed by C. W. Gear.[12] The package contains both the implicit Adams methods and the backward differentiation formulas, or the methods of C. W. Gear, as options. With Gear's methods, the increment h is restricted to small values, by the requirements of accuracy, only where the solution is relatively active. By definition, the problem is not stiff in such regions, and accuracy is achieved at minimum cost by allowing both h and the order of the method to vary. Then in regions of stiffness, where the solution is inactive, Gear's methods have the property of "stiff stability," which assures that h is no longer restricted by the small time constants, unless or until the corresponding rapidly decaying terms become active again. This property necessitates, among other things, that the method be implicit, and therefore that a system of (generally) non-linear algebraic equations be solved at each step. Moreover, stiffness dictates that a fairly powerful iteration method be used to solve this system, and the GEAR package contains variants of Newton's method (called chord methods) for this purpose. A detailed explanation of these terms and features are incorporated in the "TRANSWELL" report. [11]

Consider the components of the vector $\vec{Y}(t)$ defined by

$Y(1) = r_v(t)$ = average void radius (cm)

$Y(2) = r_{i\ell}(t)$ = average radius of an interstitial loop (cm)

$Y(3) = N_{v\ell}(t)$ = number of vacancy loops/cm^3

$Y(4) = q_{v\ell}(t)$ = vacancy concentration in vacancy loops only (at./at.)

$Y(5) = C_v(t)$ = total vacancy concentration (at./at.)

$Y(6) = C_i(t)$ = interstitial concentration (at./at.).

The governing ODE describing the time rate of change of the components of the vector $\vec{Y}(t)$ could be written explicitly as

$$\dot{Y}(1) = \frac{1}{Y(1)} \left\{ D_V Y(5) - D_I Y(6) - D_V C_V^o \exp\left(\frac{\left[\frac{2\gamma}{Y(1)} - P_g\right] b^3}{kT} \right) \right\} \tag{43}$$

$$\dot{Y}(2) = \frac{1}{b} \left\{ Z_I D_I Y(6) - Z_V D_V Y(5) + Z_V D_V C_V^o \exp\left(\frac{-[\gamma_{sf} + F_{e\ell}(Y(2))] b^2}{kT} \right) \right\} \tag{44}$$

$$\dot{Y}(3) = \frac{\varepsilon P}{\pi r_{v\ell}^2(o) b} - \frac{Y(3)}{r_{v\ell}(o) b} \left\{ Z_I D_I Y(6) - Z_V D_V Y(5) + Z_V D_V C_V^o \exp \left(\frac{[\gamma_{sf} + F_{e\ell}(r_{v\ell}(o))] b^2}{kT} \right) \right\} \tag{45}$$

$$\dot{Y}(4) = \varepsilon P - \sqrt{4\pi Y(4)Y(3)/b}\left\{Z_I D_I Y(6) - Z_V D_V Y(5) + Z_V D_V C_V^o \left(\frac{[\gamma_{sf}+F_{e\ell}(r_{v\ell})]b^2}{kT}\right)\right\} \tag{46}$$

$$\dot{Y}(5) = 4\pi Y(1)N_V D_V C_V^o \exp\left(\frac{\left[\frac{2\gamma}{Y(1)} - P_g\right]b^3}{kT}\right) + Z_V \rho_d^o D_V C_V^o + 2\pi Z_V Y(2) N_{i\ell} D_V$$

$$C_V^o \exp\left(\frac{-[\gamma_{sf}+F_{e\ell}(Y(2))]b^2}{kT}\right) + 2\pi Z_V r_{v\ell} Y(3) D_V C_V^o$$

$$\exp\left(\frac{[\gamma_{sf}+F_{e\ell}(r_{v\ell})]b^2}{kT}\right) + (1-\varepsilon)P - (4\pi Y(1)N_V D_V + Z_V \rho_d^o D_V$$

$$+ 2\pi Y(2) Z_V N_{i\ell} D_V + 2\pi r_{v\ell} Y(3) Z_V D_V) Y(5) - \alpha Y(6) Y(5) \tag{47}$$

$$\dot{Y}(6) = P - (4\pi Y(1) N_V D_I + \rho_d^o Z_I D_I + 2\pi Y(2) N_{i\ell} Z_I D_I + 2\pi r_{v\ell} Y(3) Z_I D_I) Y(6)$$

$$- \alpha Y(5) Y(6) \tag{48}$$

and $r_{v\ell} = \sqrt{Y(4)/\pi b Y(3)}$. (49)

It is noted that the time constants of the vector components Y(5) and Y(6) are much larger than the rest of the components. The main reason to order the system in the previous fashion is computational flexibility. For quasi-steady state claculations the complete set of equations are solved simultaneously until the vacancy and interstitial concentrations reach a quasi-steady state equilibrium.* Such a system, with a weak time dependence on the defect concentration is shown later in Figure (2). After the quasi-steady state is reached, the system is then reduced to a set of four equations (43-46) with continuous updating for Frenkel pair concentrations.

V. FDRT Applied to Time Independent Irradiations

FDRT is particularly sutiable for time dependent irradiation conditions, but it could be easily applied to time independent irradiations (such as neutron irradiation in fission reactors or electron irradiation in a high voltage microscope). We will study both types of irradiation here starting with the steady state defect generation case.

V. 1. 1 MeV Electron Irradiations of M316 S.S.

Since collision cascades are not produced in electron irradiated metals, vacancy loop formation is not then expected and the cascade efficiency can be set equal to zero. In this case we have only four components of the vector $\vec{Y}$; Y(1), Y(2), Y(5) and Y(6).

The parameters for M316 steel (solution treated) listed in Table 1 were adopted for these calculations:[10]

---

*Quasi-steady state point defect equilibrium is reached when the sink structure has a weak time dependence, and could be considered fixed within a certain time interval.

Table 1

Summary of Materials Constants For 316 SS Void Growth Calculations

Surface Energy, γ	$= 1.25 \times 10^{15}$ ev cm^{-2}
Vacancy formation Energy, E_f^v	= 1.6 ev
Vacancy migration Energy, E_m^v	= 1.3 ev
Interstitial formation Energy, E_i^f	= 4.0 ev
Interstitial migration Energy, E_i^m	= 0.2 ev
Vacancy diffusivity, D_v^o	$= 0.6$ cm^2 s^{-1}
$\frac{\text{recombination coefficient}}{\text{interstitial diffusion coefficient}}$, $\frac{\alpha}{D_i}$	$= 10^{16}$ cm^{-2}
stacking fault energy, γ_{sf}	$= 9.4 \times 10^{12}$ ev cm^{-2}
deformation produced dislocation density, ρ_d^o	$= 10^8$ cm^{-2}
Burgers vector, b	$= 2 \times 10^{-8}$ cm
dislocation bias for vacancies, Z_v	= 1.00
dislocation bias for interstitials, Z_i	= 1.08
Effective modulus, $\mu' = \frac{\mu}{1-\nu}$	$= 4 \times 10^{11}$ dyne cm^{-2}

To represent nucleation conditions, temperature dependent void and interstitial loop concentrations were used. The temperature dependence of void concentration (eq. 50) is based on experimental observation[13] while the interstitial loop concentration (eq. 51) is a suitable fit governed by the reasonable agreement between theory and experiment.[10]

$$N_v = 6.5 \times 10^8 \exp(1.0/kT) \tag{50}$$

$$N_{il} = 6.7 \times 10^{-3} \exp(2.8/kT) \, . \tag{51}$$

The four equations for Y(2), Y(3), Y(5) and Y(6) are then solved numerically with the initial conditions

$$r_v(0) = 10 \text{ Å} \tag{52}$$

$$r_{i\ell}(0) = \sqrt{4r_v^3(0) \, N_v/3bN_{i\ell}}, \tag{53}$$

$$N_{v\ell}(0) = 0, \tag{54}$$

$$q_{v\ell}(0) = 0, \tag{55}$$

$$P_g(0) < 2\gamma/r_v(0) \, . \tag{56}$$

The last condition represents a void slightly larger than an equilibrium gas bubble and is necessary because a surge of interstitials will rush to the void shortly after the beginning of irradiation tending to shrink its size. An equivalent condition to (56) is continuous re-emission of helium atoms from the void to maintain an equilibrium gas bubble.

At irradiation times of the order of the first few microseconds, neither interstitials nor vacancies are mobile enough to migrate to neutral and biased sinks. Also their concentrations will be so low that the mutual recombination is neglected. Under these conditions the rate of change of the concentration of vacancies and interstitials is almost equal to the production rate. In Figure (1) the initial slope of $C_i(t)$ and $C_v(t)$ is about 5×10^{-3} at/at/sec, the actual production rate. The build-up of the interstitial concentration coupled with their high mobility will cause the interstitial sink removal rate to be large at about 10^{-5} seconds. The concurrent build-up of the vacancy concentration also produces a high recombination rate. Consequently the total interstitial concentration has to pass through a maximum and decrease in value as a function of time. As time progresses, the high vacancy concentration and the mobility of vacancies will produce a vacancy sink removal rate which increases with time. After a few vacancy mean lifetimes the vacancy concentration will decrease with time producing the broad maximum as shown in Figure (1). The recombination rate is a strong function of the concentration (quadratic) while the sink removal rates are linear. After an accumulated dose of

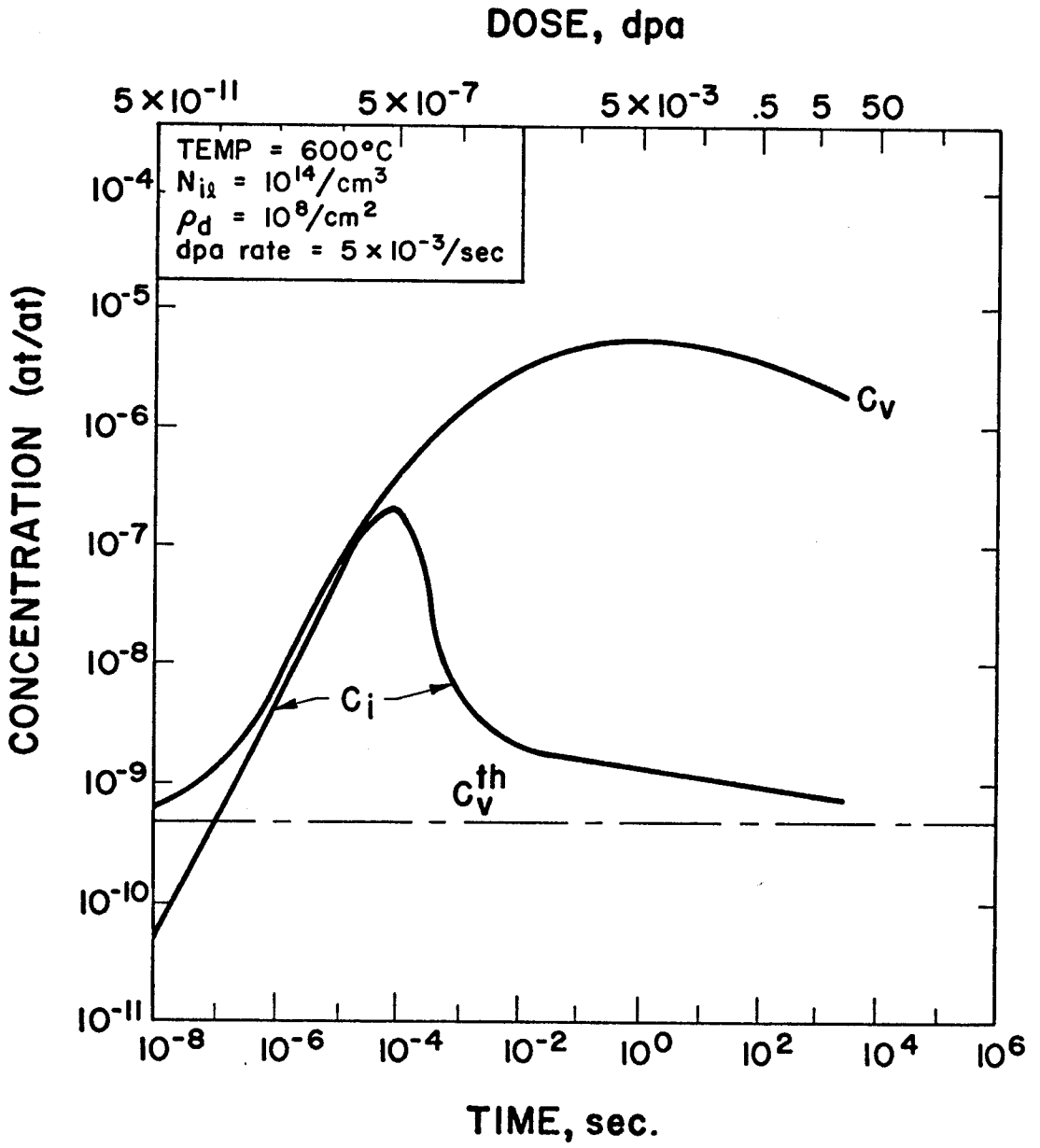

Fig. (1) Point Defect Concentrations in electron irradiated M316 S.S. using the Fully Dynamic Rate Theory (FDRT)

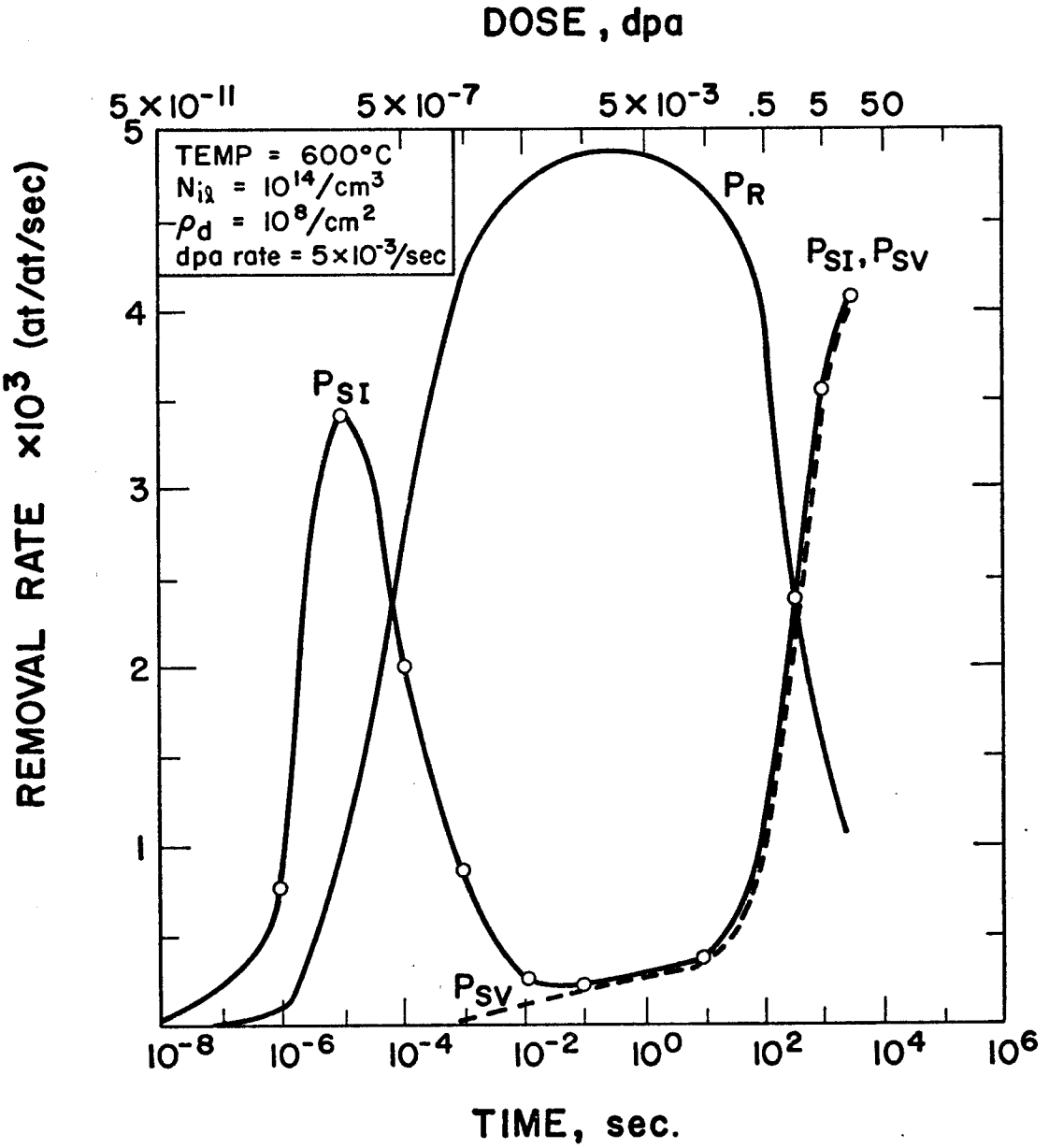

Fig. (2) Removal Rates P_R, P_{SI}, P_{SV} in electron irradiated M316 S.S. using the Fully Dynamic Rate Theory (FDRT)

0.01 - 0.1 dpa the point defect concentrations will decay slowly with time which makes the recombination rate also decrease to the point where the various sink removal rates are the dominant loss mechanism. The increase of the sink removal rates is due to the growth of voids and interstitial loops.

IV. 2. 22 MeV C^{++} Ion Bombardment of M316 S.S.

The swelling behavior of solution treated M316 stainless steel was intensively studied because of its commercial importance. Mazey, Nelson and Hudson[14] and Williams[15] irradiated samples of S. T. M316 S.S. with 22 MeV C^{++} ions and determined the dislocation densities, average void diameter and final swelling as a function of temperature. An attempt was made to duplicate this data using FDRT via the TRANSWELL[11] code. The stainless steel materials parameters were taken as described in table 1.

Void and interstitial loop concentrations at the end of the nucleation phase and the start of the growth phase were taken as

$$N_v = 3.15 \times 10^{11} \exp(0.625/kT) \qquad (57)$$

$$N_{il} = 1.34 \times 10^{-4} \exp(2.8/kT) \qquad (58)$$

and the fraction of vacancies forming vacancy loops (ε) is taken as 0.044.

Figure (3) shows the swelling predicted by the FDRT theory and that measured in the experiment. At low temperatures the vacancies are immobile and high recombination rates are expected so that a smaller fraction of point defects migrate to biased and neutral sinks. This will tend to suppress swelling. At intermediate temperatures (around 550-650°C) vacancies are very mobile and sink removal rates have in increased importance leading to higher values of swelling. At high temperatures (higher than 650°C) the irradiation produced vacancy concentration will be comparable to or smaller than the thermal vacancy concentration. In this temperature regime the irradiation is unable to cause high swelling values due to high vacancy emission rates and low dislocation loop densities.

The temperature dependence of the average void size at 40 dpa is shown in Figure (4). There is rather good agreement between experimentally measured void diameters and those predicted theoretically over a wide range of temperatures.

The predicted dislocation density is much higher than observed experimentally as shown in Figure (5). The theory predicts that the bulk of the dislocation sink density is in the form of small vacancy loops. However, since vacancy loops are expected to form with very small dimensions, in the order of tens of angstroms, the experimental observation of vacancy loops will be difficult. Bearing in mind these experimental difficulties, it is felt that experimental and theoretical dislocation densities could show general agreement over a wide range of doses.

The predicted dose dependence of the average void and interstitial loop radii for 22 MeV C^{++} irradiated S.S. are shown in Figure (6). The dose dependence of the void and loop radii is not strong at low

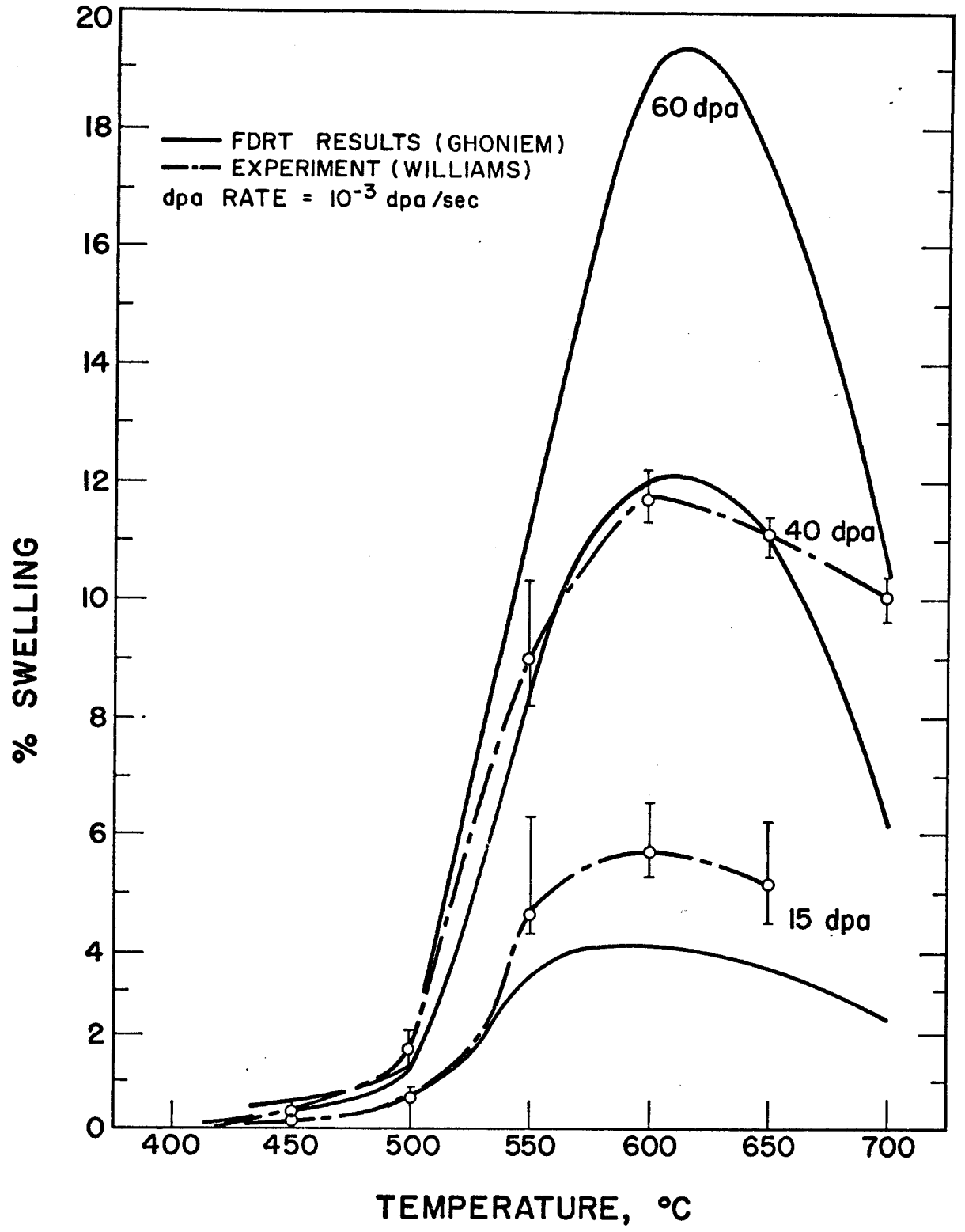

Fig. (3) COMPARISON BETWEEN THE FULLY DYNAMIC RATE THEORY (FDRT) AND EXPERIMENTAL RESULTS FROM T.M. WILLIAMS (AERE HARWELL). THE TEMPERATURE DEPENDENCE OF VOID SWELLING IN M316 S.S. IRRADIATED WITH 22 MeV C^{++} IONS.

Fig. (4) COMPARISON BETWEEN THE FULLY DYNAMIC RATE THEORY (FDRT) AND EXPERIMENTAL RESULTS FROM T.M. WILLIAMS (AERE HARWELL). THE TEMPERATURE DEPENDENCE OF VOID DIAMETER AS A FUNCTION OF TEMPERATURE AT 40 dpa IN SOLUTION TREATED M316 S.S. IRRADIATED WITH 22 MeV C^{++} IONS.

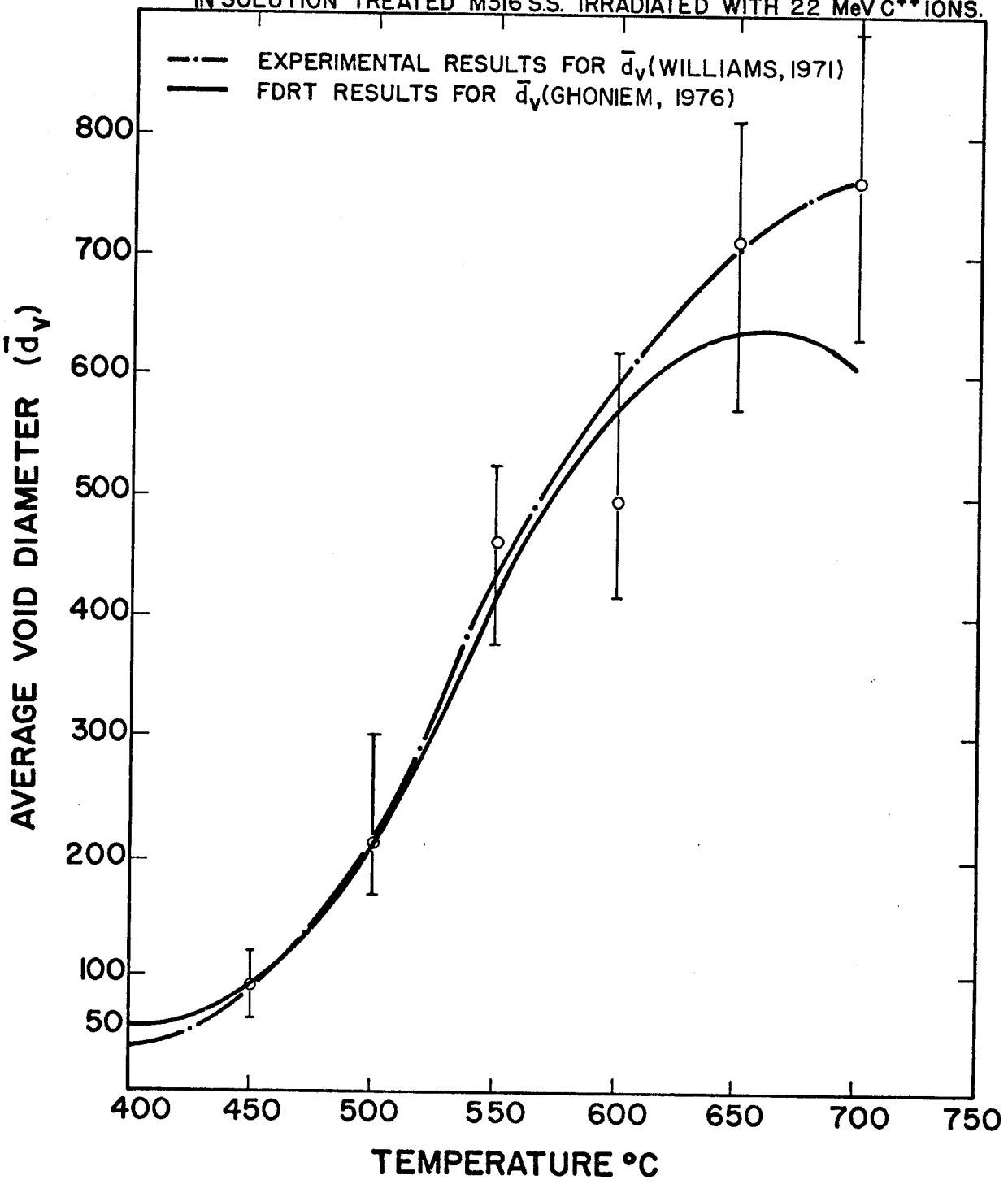

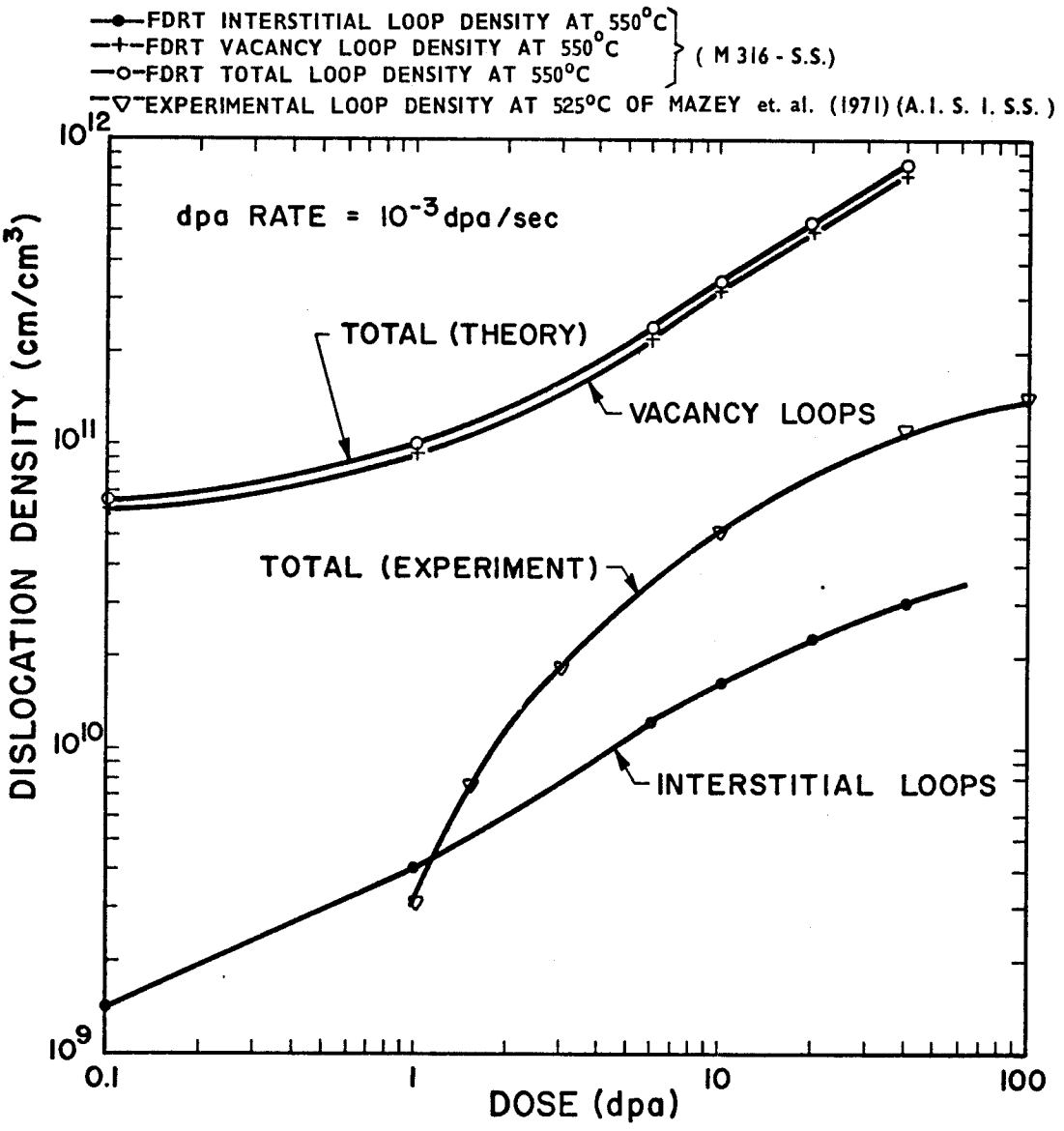

Fig. (5) THEORETICAL AND EXPERIMENTAL DOSE DEPENDENCE OF DISLOCATION DENSITIES DURING 22 MeV C^{++} IRRADIATION.

temperatures because of the high recombination rate. Therefore a smaller fraction of point defects will migrate to sinks to cause swelling and loop growth. This region is characterized by low nucleation densities and large growth rates of voids and interstitial loops, hence higher swelling values. An example of this behavior is illustrated in Figure (6) for the growth of voids and interstitial loops at 600°C. Shortly after the incubation dose the average void radius starts to increase rapidly. As irradiation proceeds, the void (neutral) sink strength increases rendering the dislocation density somewhat less effective in removing point defects. The impact of the growing void sink strength is to decrease the average void radius growth rate as a function of dose. It is also observed that the average interstitial loop growth follows that of the average void growth. One would expect this behavior because excess vacancies migrate to voids while excess interstitials migrate to interstitial dislocation loops.

Vacancy dislocation loops have a great effect on reducing the swelling during neutron or heavy ion irradiations. Their effect is to reduce the total production rate of free vacnacies and to act as an additional biased sink for interstitials. Initially the number of vacancy loops increases linearly with time (figure 7). The slope is temperature independent since the fraction of vacancies retained in vacancy loops was assumed to be temperature independent. However, the vacancy emission rates are both temperature and time dependent and eventually an approach to an

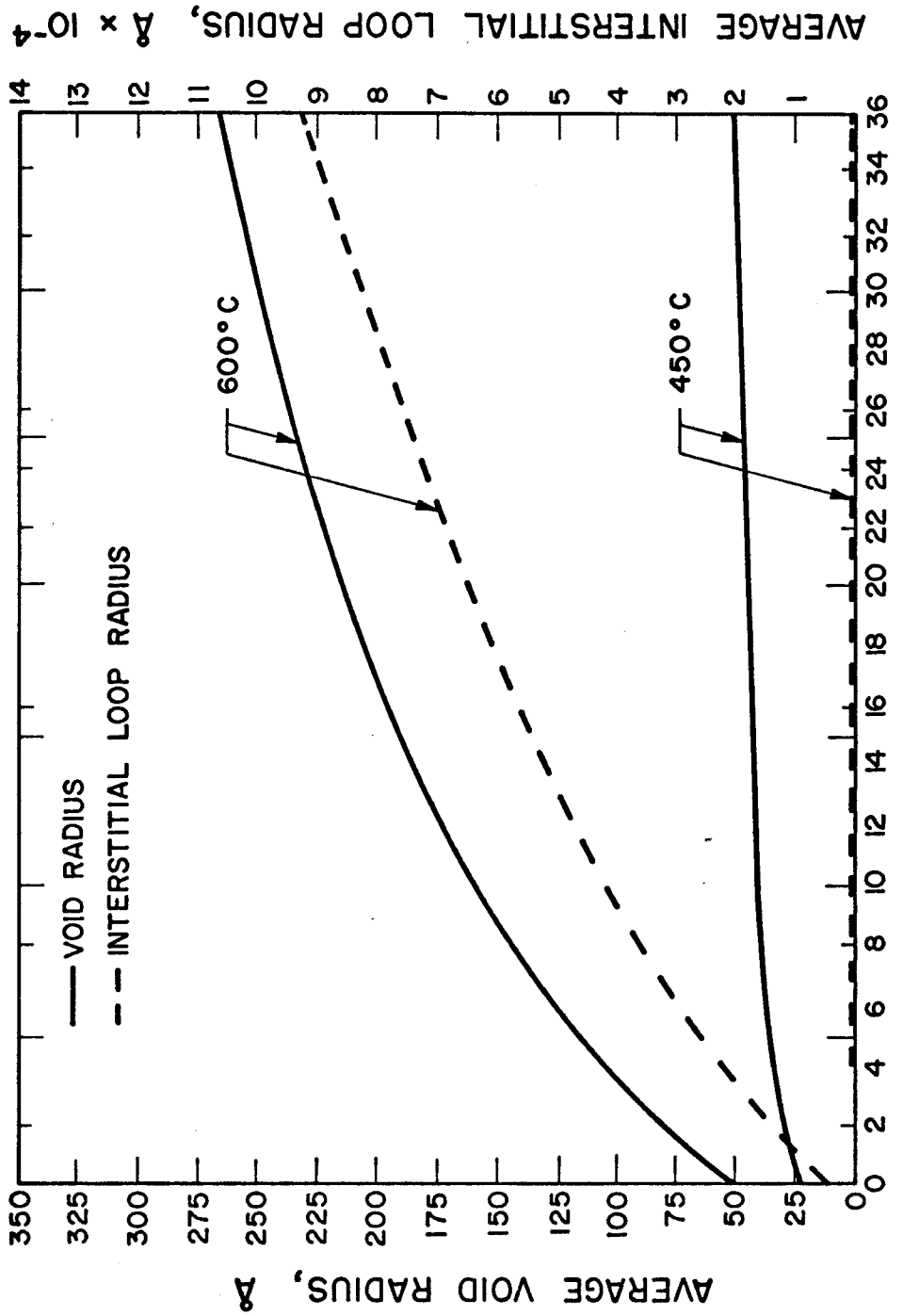

Fig. (6) THE PREDICTED DOSE DEPENDENCE OF THE AVERAGE VOID AND INTERSTITIAL LOOP RADII FOR 22 MeV C^{++} IRRADIATED S.S. dpa rate = 10^{-2} dpa/sec

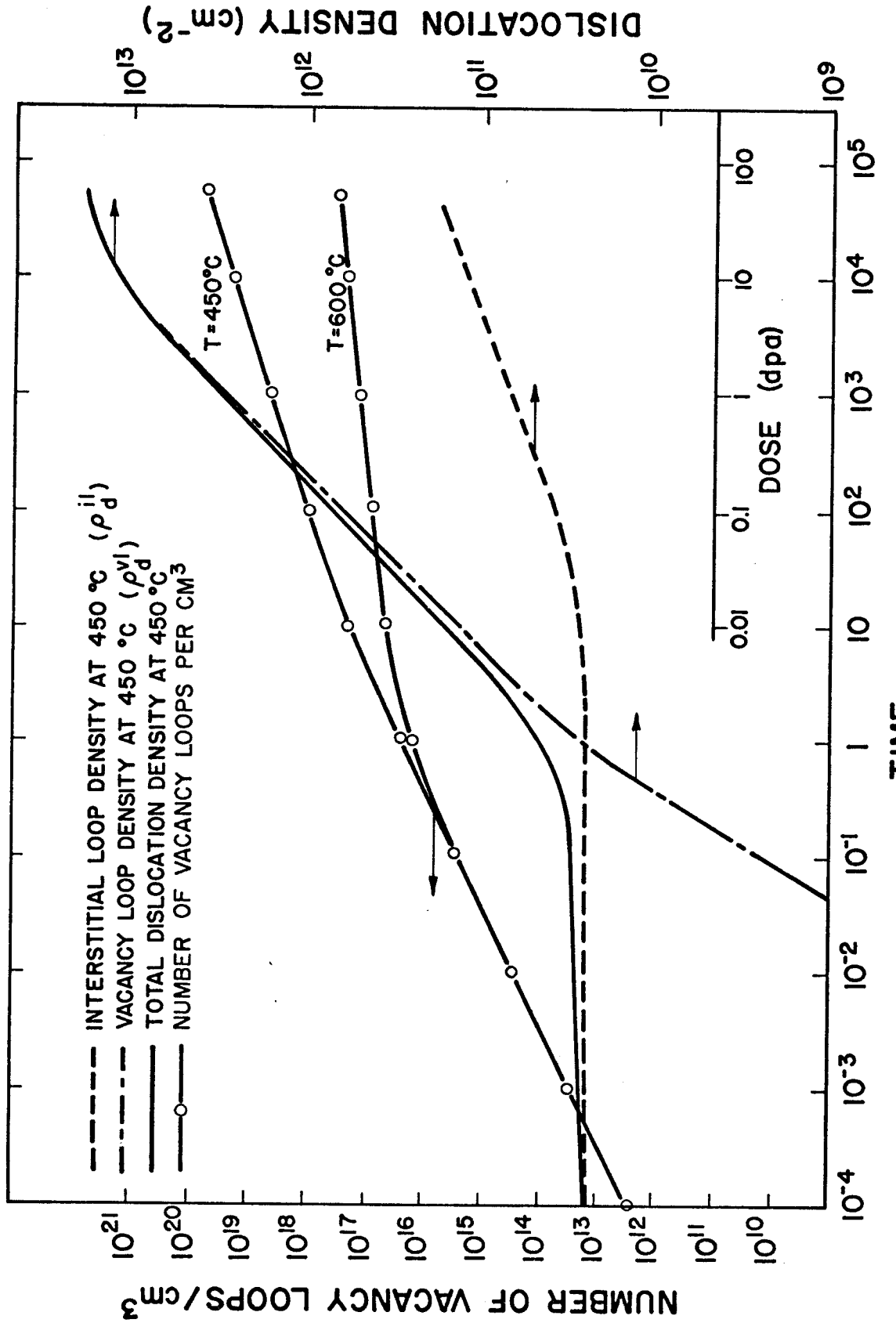

Fig. (7) THE DOSE DEPENDENCE OF DISLOCATION DENSITY AND VACANCY LOOP CONCENTRATION FOR 22 MeV C^{++} IRRADIATED S.S. dpa RATE = 10^{-3} dpa/sec

equilibrium value is reached. The results shown here in Figure (7) agree with the theoretical values of Bullough, et al.[10]. The only discrepancy is at short periods of times which is probably due to the transient conditions treated here versus quasi-steady state approximation used in their work. However, this graph shows the necessity to include recovery of dislocations as a part of the mathematical simulation because at low temperatures and high doses the dislocation densities approach an unrealistic level of 10^{13} cm^{-2}.

VI. FDRT Applied to Pulsed Irradiations

Thus far we have calibrated the theory against heavy ion irradiation under time independent conditions. The main purpose of extending the rate theory, however, is to be able to apply it reliably to time-dependent situations. To fully assess the effects of pulsed irradiation on the behavior and response of metals, a wide range of pulsing schemes have to be investigated. However, in this paper we will only consider one example from a laser fusion reactor.

VI. 1. Laser Fusion Pulsed System

The example studied here applies to a preliminary version of the Laser Fusion Reactor presented elsewhere.[24] The materials behavior under the conditions described here are not necessarily typical of pulsed systems in general. This is because the behavior of a metal subjected to pulsed irradiation will depend on many factors:

1) Temperature

2) Dislocation and void densities

3) Impurity content

4) Crystal structure

5) Gaseous content

6) Bombarding particle

7) Cumulative damage in the pulse

8) Pulse width

9) Damage rate during the pulse

10) Time interval between pulses

In this study we consider solution treated stainless steel with the parameters given in Section IV. 1. A 100 MJ microexplosion in the center of a 3.5 m radius cavity is analyzed and the integrated fluence in each microexplosion is found to be 3.55×10^{19} neutron/pulse. A graphite liner of 1.5 cm thickness is placed 1 cm in front of a stainless steel wall of 0.1 cm thickness. The neutronic calculations used 25 neutron energy groups and 21 gamma energy groups and a time dependent version of ANISN[25] is used. A cumulative dpa of $\sim 10^{-7}$ per pulse is generated in stainless steel and an approximate damage pulse is considered to be

$$\text{dpa rate} = 10 \text{ dpa/sec } 0 \leq t \leq 10^{-8} \text{ sec},$$
$$= 0 \text{ dpa/sec } 10^{-8} < t < \infty \text{ sec.}^{*}$$

VI. 2. Analysis and Results

A normal procedure in engineering analysis is to study what is considered to be the worst case. The conditions studied here correspond to a complete previous nucleation of voids and interstitial loops as given by equations (57) and (58).

---

* In the reactor design of reference 24 the pulse was assumed to be repeated every 30 milliseconds.

A cavity of 40 Å radius in the original array is assumed and we allow for growth of equilibrium bubble embryoes to voids. Theoretical studies (16,17) on the other hand suggested lower nucleation rates under pulsed irradiation compared to steady irradiation conditions, but we will not treat that question here.

Figure (8) shows the time dependence of the point defect recombination rate ($P_R(t)$), the interstitial total sink leakage rate ($P_{SI}(t)$), and the vacancy total sink leakage rate ($P_{SV})t)$) during one pulse and up to 10 seconds after the pulse.

During the irradiation pulse the rapid buildup of point defect concentrations produce a large mutual recombination rate. Consequently, it is advantageous to design for short pulses of high displacement rates because a larger number of vacancies and interstitials are removed by recombination and thus swelling could be reduced. Due to the high mobility of interstitials, the interstitial sink removal rate ($P_{SI}(t)$) increases with time during the pulse. At the end of the irradiation pulse the recombination rate and the interstitial sink removal rate will drop sharply. Around a vacancy mean lifetime, the vacancy sink removal rate ($P_{SV}(t)$) is the only active sink and hence it reduces the vacancy concentration as shown in Figure (8).

Pulsing the metal changes its microstructure gradually. The vacancy loop idslocation density increases during the pulse adding to the total dislocation density, but obviously many pulses would be needed before significant changes can occur.

REMOVAL RATES OF POINT DEFECTS FOR 316 STEEL UNDER AN IRRADIATION PULSE.

FIG. (8)

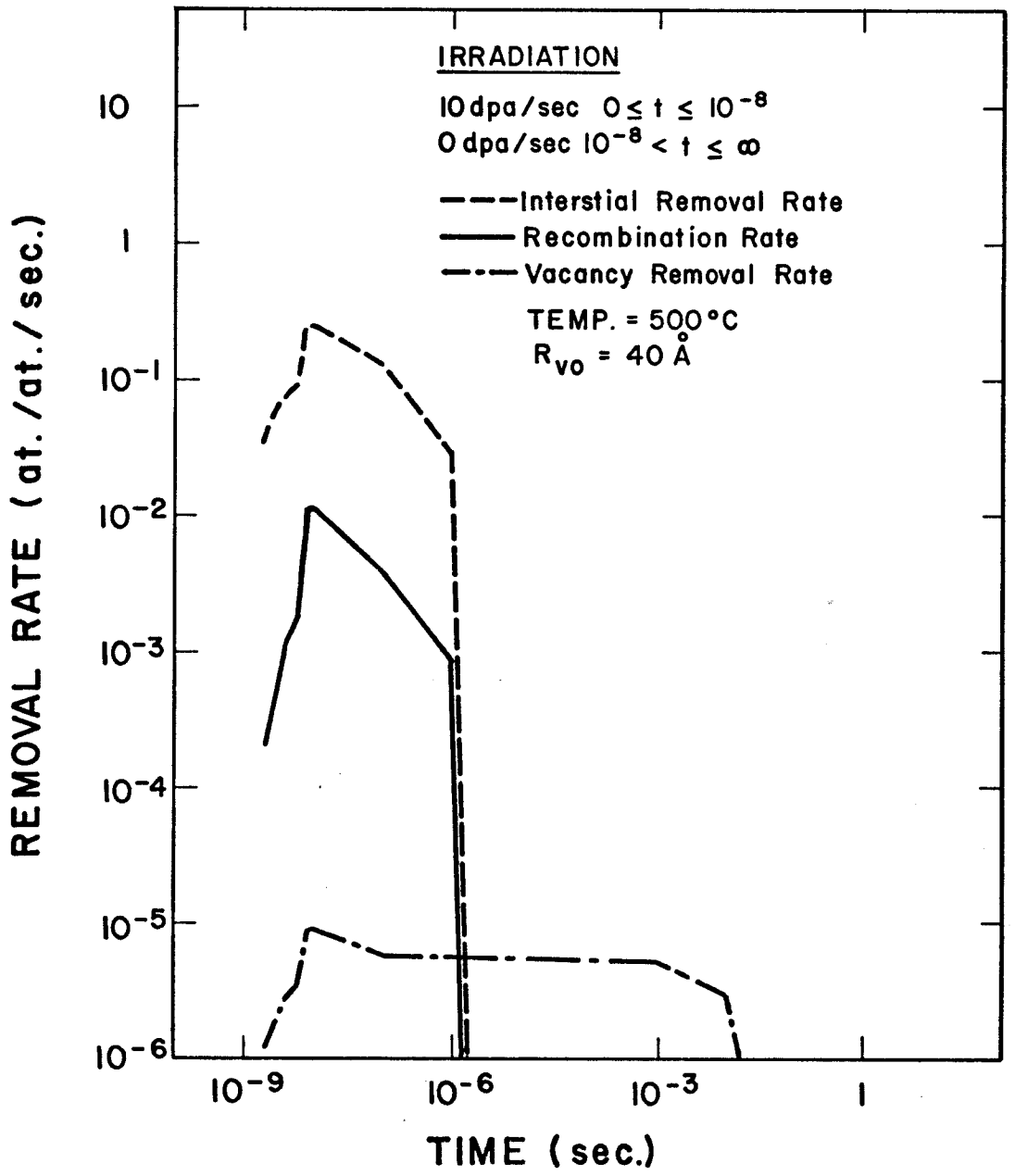

Interstitial loop dislocation density changes also during and after the irradiation pulse mainly because of the slight changes that take place to the average loop radius. The total dislocation density will change accordingly.

The vacancy and interstitial concentrations in a pulsed system are shown in Figures (9, 10, 11, 12) for various irradiation temperatures. A common characteristic of the point defect time behavior is an approximately constant rate of change during the pulse. This rate of change is about the dpa rate (10 dpa/sec in this case). However, the vacancy concentration during the pulse is a little less than the interstitial concentration because of vacancy loop formation during the irradiation pulse. Interstitials, being very mobile, will have a sharply decreasing concentration right after the end of the pulse. The vacancy concentration maintains the value acquired during the pulse ($\sim 10^{-7}$ dpa) for a much longer time before dropping around the main vacancy lifetime.

A peculiar behavior of the system is that it almost preserves the timewise decay behavior of point defects. Increasing the temperature decreases the dislocation density, but increases the point defect diffusion coefficients. These two processes are both exponential in nature with respect to temperature and result in an "almost" temperature invariant time constant for vacancy and interstitial concentrations.

After the end of the irradiation pulse, the flux of interstitials to the void is higher than the flux of vacancies and the void radius decreases rapidly. Around a vacancy mean lifetime the vacancy flux to the void gives rise to an increase in the void size.

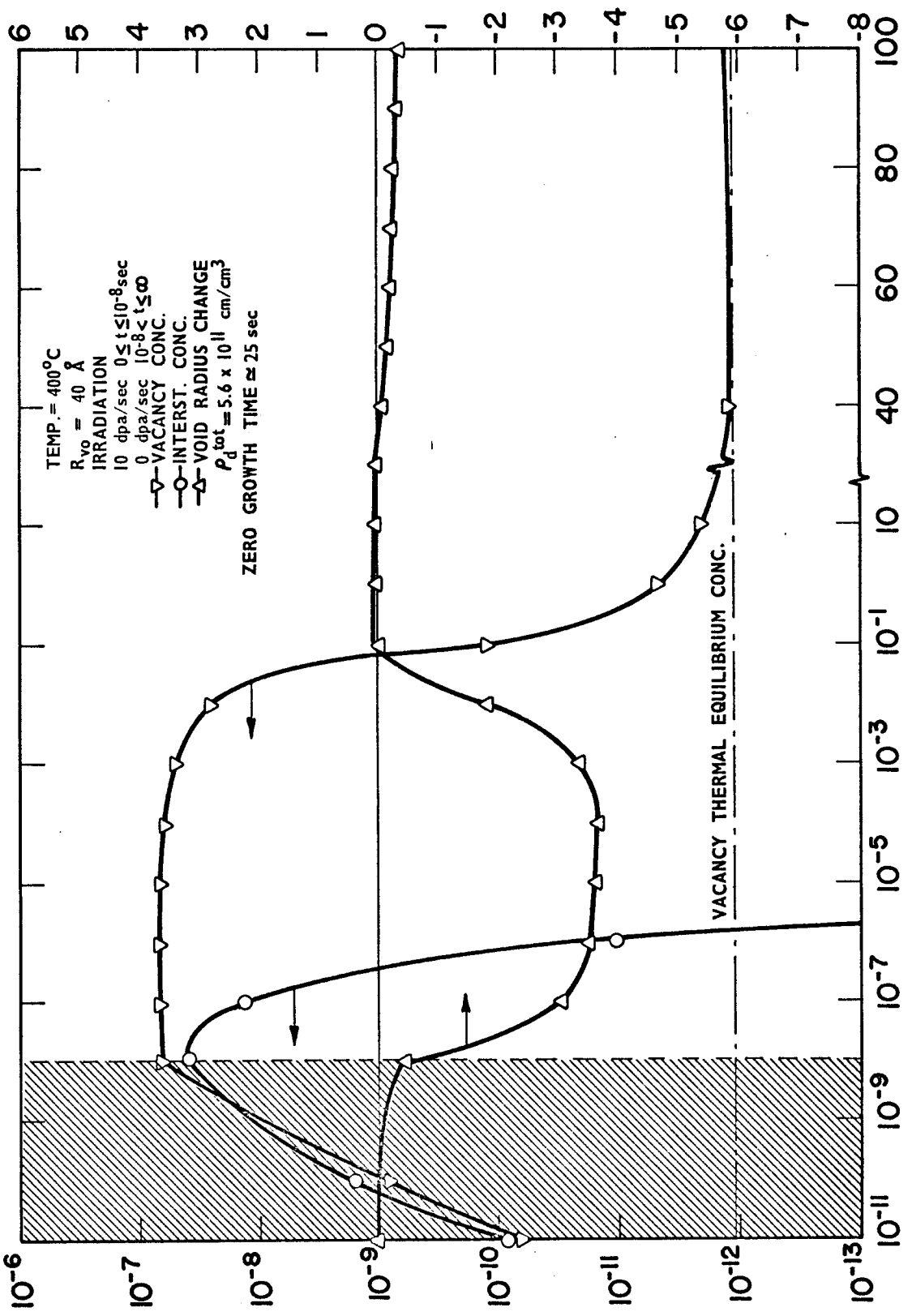

Fig.(9) POINT DEFECT CONCENTRATIONS AND CHANGE IN VOID RADIUS AS A FUNCTION OF TIME DURING AND AFTER AN IRRADIATION PULSE AT 400 °C FOR S.T. 316 S.S.

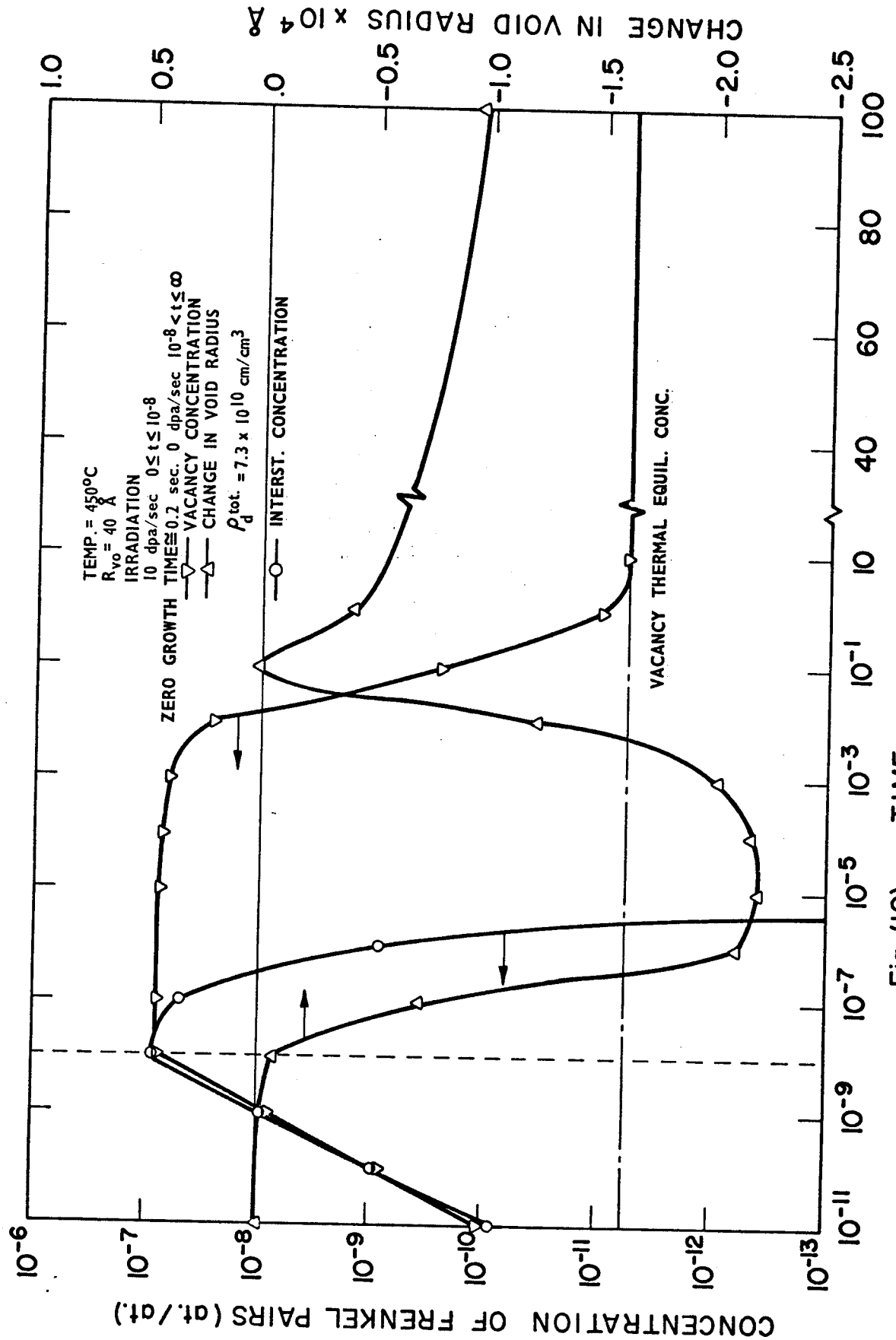
CHANGE IN VOID RADIUS x 10⁴ Å
1.0
0.5
0
-0.5
-1.0
-1.5
-2.0
-2.5
TEMP. = 450°C
R_vo = 40 Å
IRRADIATION
10 dpa/sec 0≤t≤10⁻⁸
ZERO GROWTH TIME≅0.2 sec. 0 dpa/sec 10⁻⁸<t≤∞
VACANCY CONCENTRATION
CHANGE IN VOID RADIUS
P_d^tot. = 7.3 x 10¹⁰ cm/cm³
INTERST. CONCENTRATION
VACANCY THERMAL EQUIL. CONC.
CONCENTRATION OF FRENKEL PAIRS (at./at.)
10⁻⁶
10⁻⁷
10⁻⁸
10⁻⁹
10⁻¹⁰
10⁻¹¹
10⁻¹²
10⁻¹³
10⁻¹¹
10⁻⁹
10⁻⁷
10⁻⁵
10⁻³
10⁻¹
10
40
60
80
100
TIME, sec.

Fig. (10)

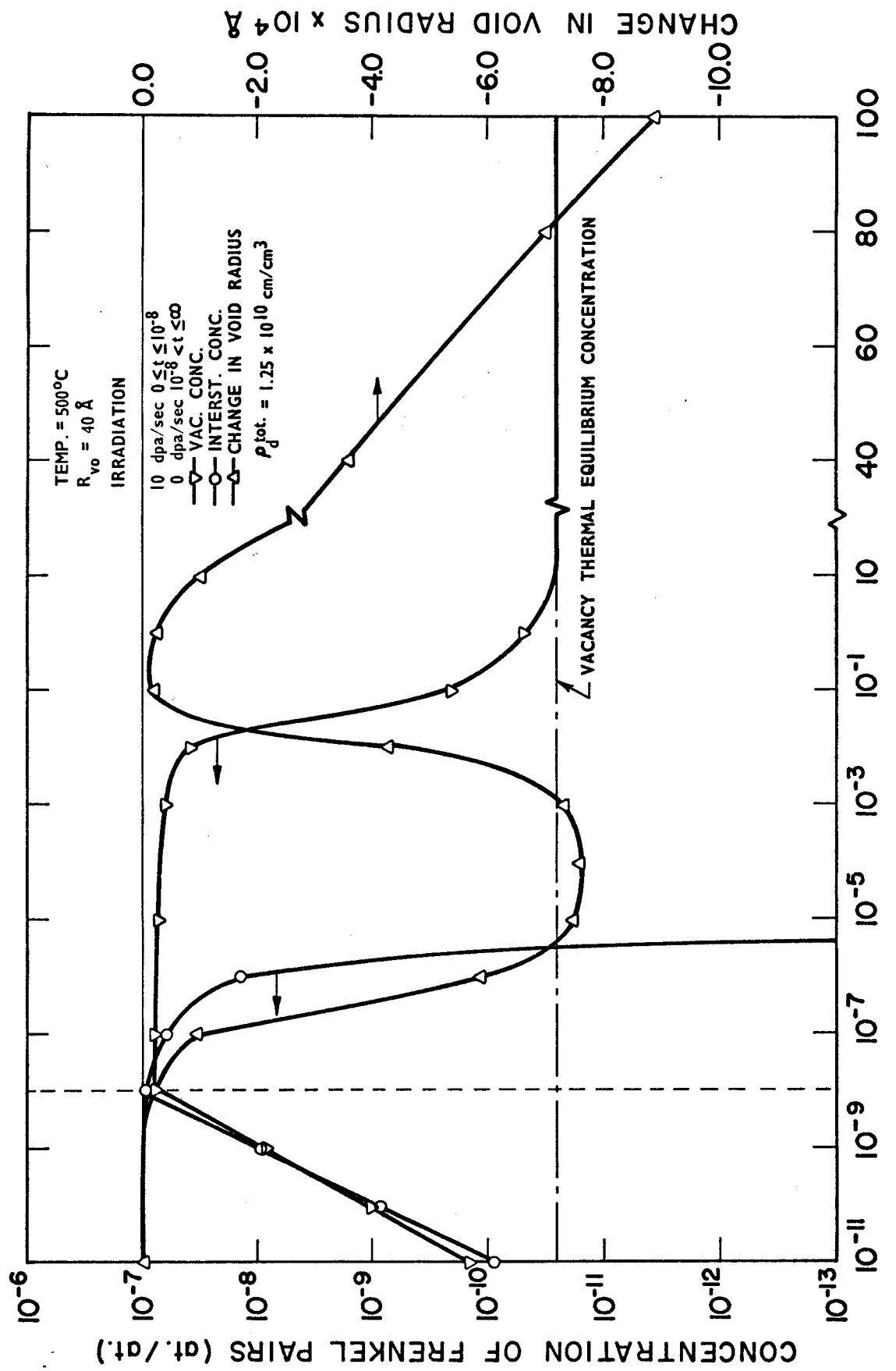
CHANGE IN VOID RADIUS x 10⁴ Å
0.0
-2.0
-4.0
-6.0
-8.0
-10.0
TEMP. = 500°C
R_Vo = 40 Å
IRRADIATION
10 dpa/sec 0 ≤ t ≤ 10⁻⁸
0 dpa/sec 10⁻⁸ < t ≤ ∞
VAC. CONC.
INTERST. CONC.
CHANGE IN VOID RADIUS
ρ_d^tot. = 1.25 x 10¹⁰ cm/cm³
VACANCY THERMAL EQUILIBRIUM CONCENTRATION
CONCENTRATION OF FRENKEL PAIRS (at./at.)
10⁻⁶
10⁻⁷
10⁻⁸
10⁻⁹
10⁻¹⁰
10⁻¹¹
10⁻¹²
10⁻¹³
10⁻¹¹
10⁻⁹
10⁻⁷
10⁻⁵
10⁻³
10⁻¹
10
40
60
80
100
TIME, sec.

Fig. (11)

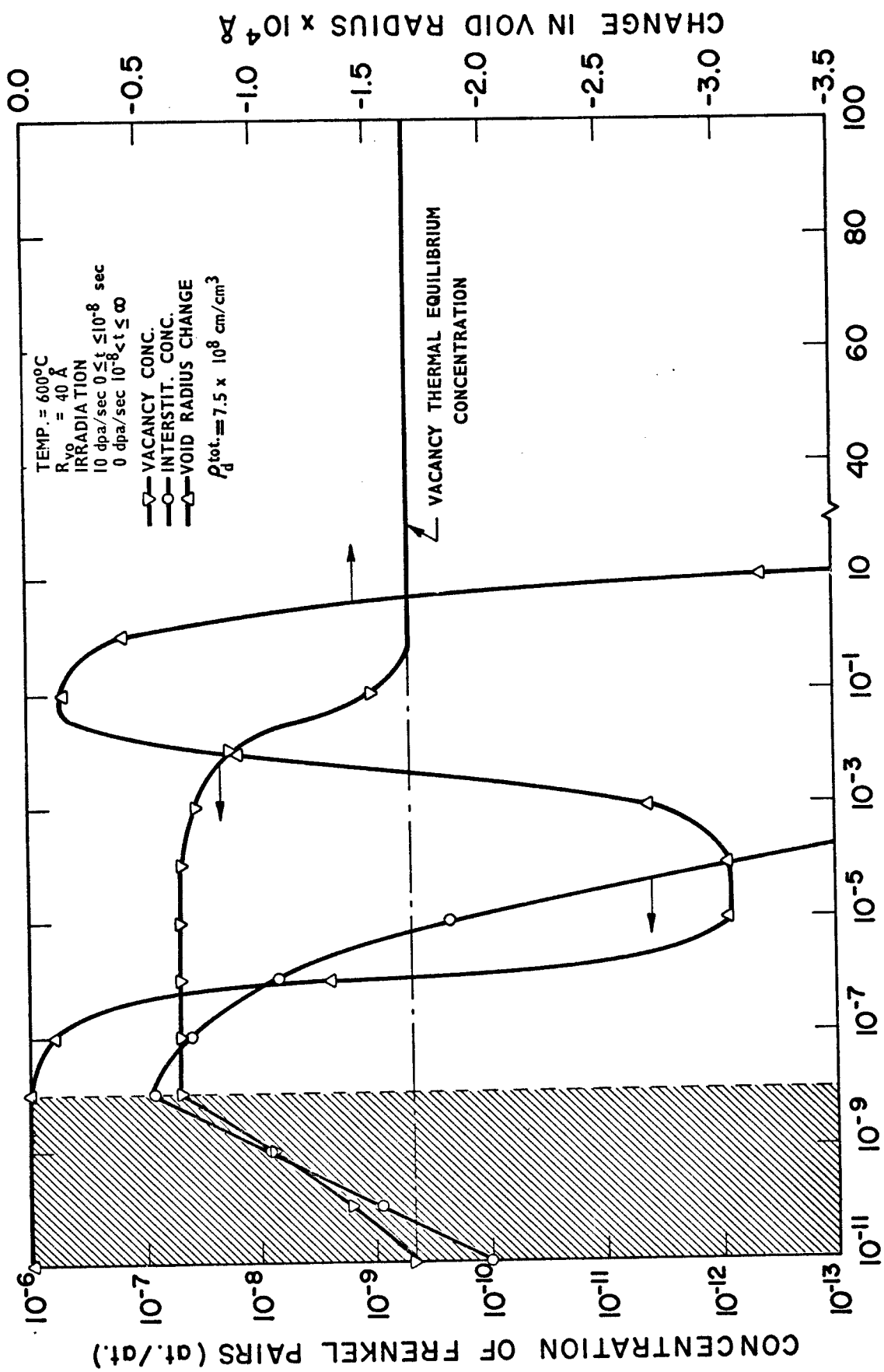

Fig. (12) POINT DEFECT CONCENTRATION AND CHANGE IN VOID RADIUS AS A FUNCTION OF TIME DURING AND AFTER AN IRRADIATION PULSE AT 600 °C FOR S.T. 316 S.S.

Void Annealing in Metals

At a given temperature T, the vacancy concentration at the void, C_v, is given by

$$C_v/C^o = \exp\{(\frac{\partial F}{\partial n})/kT\} \tag{59}$$

where $\frac{\partial F}{\partial n}$ is the change in energy of the configuration per vacancy emitted, and C^o the equilibrium concentration of vacancies. For a spherical hole in an infinite isotropic solid, the emission depends on the surface energy of the void, the elastic strain energy in the surrounding metal, the applied hydrostatic stress, and the pressure caused by trapped gas atoms inside.

Generalizing the analyses given in (5, 18, 19); one can write the following expressions:

$$\frac{\partial F}{\partial n} = F_m \Omega \tag{60}$$

where Ω is the atomic volume. Here F_m is the mechanical force per unit surface area acting on a vacancy at the void surface.

$$F_m = P + \frac{2\gamma}{r_v} + \frac{\gamma^2}{2\mu r_v^2} - P_g \ . \tag{61}$$

Here P is the hydrostatic pressure, γ the surface energy, r_v the void radius, μ the shear modulus, and Pg the gas pressure.

The gas pressure is always expressed in terms of the number of gas atoms and void radius. If the perfect gas law is used, one gets:

$$P_g = \frac{3n_g kT}{4\pi r_v^3} \ . \tag{62}$$

While if Van der Waals law is assumed to hold,[20] one gets:

$$P_g = \frac{n_g kT}{(4/3\pi r_v^3 - an_g)} - \frac{bn_g^2}{16/9\pi^2 r_v^6} \qquad (63)$$

This formulation is useful in studying the general situation where gas atoms are trapped in voids and where stress waves accompany the damage production.

Although the principal concern in modeling void behavior has been void growth during irradiation, some consideration has been given to the response of voids during post irradiation annealing.[21,22] Annealing in the absence of irradiation is of interest for the practical reason that some CTR first wall materials will be subject to periods of irradiation and post irradiation annealing. Furthermore, void annealing experiments present a unique opportunity to study void kinetic behavior in the absence of self interstitials and in the presence of a low vacancy supersaturation.

Figures (9,10,11,12) show the essential features of void kinetics due to an irradiation pulse. At 400°C, after gaining excess vacancies due to the irradiation pulse, the void begins to slowly anneal out this excess. For example, it takes the void a relatively long time (~25 seconds in this case) to achieve a zero growth condition. For voids to start emitting vacancies, the average vacancy concentration at its surface should be greater than the average vacancy concentration in the matrix. The void will thermally emit vacancies if the following relationship is satisfied.

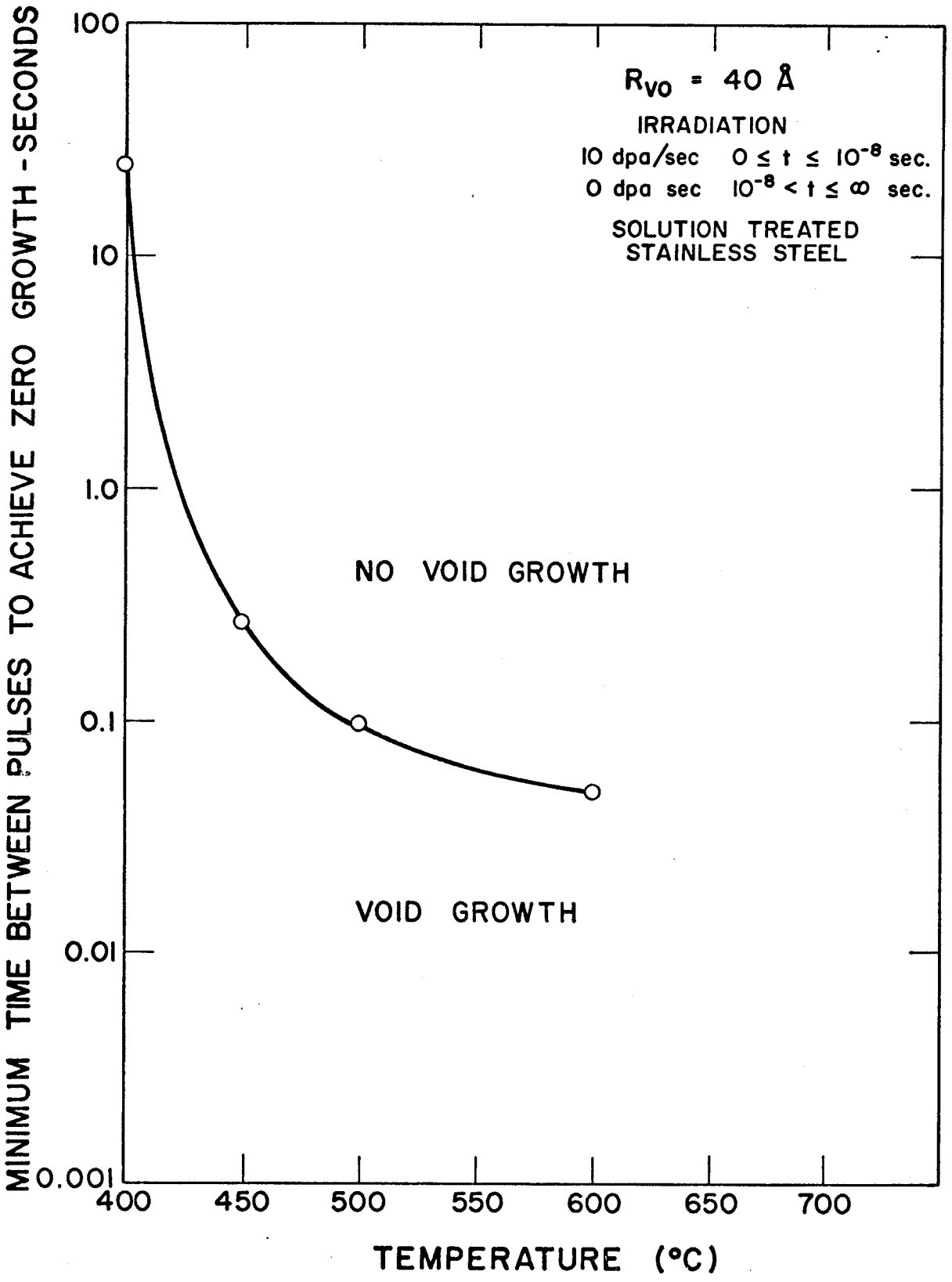

Fig. (13)

Growth and No growth regimes for a 40 Å radius void under pulsed irradiation.

$$C_V(t) \leq C_V^o \exp\{(\frac{\partial F}{\partial n})/kT\} \qquad (64)$$

This time is shorter for higher temperatures and lower average concentrations. The behavior could be followed through Figures (9,10,11,12).

Figure (13) shows the minimum time between the pulses to achieve zero growth conditions as a function of temperature. The important temperature regime of operation that emerges from this picture is between 450°C and 550°C. A repetition rate of 5-20 pulses per sec. will produce zero swelling while higher pulse rates will cause growth and lower pulse rates cause less.

V. 3. Details of the Rate Processes

It is shown that appropriate irradiation procedures can eliminate many factors that contribute to metal swelling. It will serve to give more insight to the relative importance of different rate processes in the metal under consideration. Details of these processes will be given here during the pulse and around a vacancy mean lifetime.

Examples of the various defect properties during and after the 10 ns damage pulse are given in tables (2) and (3). The data in tables (2) and (3) refers to the following conditions:

Temperature = 500°C

Vacancy Thermal Equilibrium Concentration = 6.075×10^{-11} at./at.

Interstitial Thermal Equilibrium Concentration = 8.316×10^{-21} at./at.

The tables are too detailed for a complete discussion at this time and the reader is urged to examine them in depth taking particular note of the vacancy and interstitial concentrations, leakage rates of both defects, recombination rates, and rate of growth of both vacancy and interstitial clusters.

Table (2)

Time		= 2×10^{-9} sec
Total Dose		= 2×10^{-8} dpa
(1)	Average concentrations of point defects (at/at)	
	Average concentration of vacancies	= 1.916×10^{-8}
	Average concentration of interstitials	= 1.997×10^{-8}
(2)	Leakage constants of Frenkiel Pairs to different sinks (sec^{-1})	
(2-A)	Leakage constants of vacancies to sinks	
	Leakage constant of vacancies to all sinks	= 60.24
	Leakage constant of vacancies to dislocations	= 23.76
	Leakage constant of vacancies to voids	= 36.48
(2-B)	Leakage constant of interstitials to sinks	
	Leakage constant of interstitials to all sinks	= 1.592×10^{6}
	Leakage constant of interstitials to dislocations	= 6.575×10^{5}
	Leakage constant of interstitials to voids	= 9.345×10^{5}
(3)	Emission rates of vacancies (at/at/sec)	
	Emission rate from vacancy loops	= 8.411×10^{-14}
	Emission rate from interstitial loops	= 7.955×10^{-10}
	Emission rate from voids	= 2.857×10^{-9}
	Emission rate from dislocations	= 7.168×10^{-12}
	Total emission rate of vacancies	= 3.659×10^{-9}
(4)	Rate of recombination of vacancies and interstitials (at/at/sec)	= 2.041×10^{-4}
(5)	Leakage rate of vacancies to all sinks (at/at/sec)	= 1.196×10^{-6}
(6)	Leakage rate of interstitials to all sinks (at/at/sec)	= 3.295×10^{-2}
(7)	Radii of voids and loops in angstroms	
	Void Radius	= 40.
	Interstitial loop radius	= 825.5
(8)	Rate of change of void and loops radii in cm/sec	
	Rate of change of void radius	= -2.569×10^{-6}
	Rate of change of interstitial loop radius	= 5.55×10^{-5}
(9)	Number of vacancy loops and fraction of vacancies retained in them	
	Number of vacancy loops	= 6.225×10^{11}
	Fraction of vacancies in loops	= 8.8×10^{-10}
(10)	Changes of initial radii of void and interstitial loop in ang.	
	Change in loop radius (RIL-RILO)	= 5.357×10^{-6}
	Change in void radius (RV-RVO)	= -2.48×10^{-7}

Table (3)

While at longer times the following values are obtained

Time		= 10. sec
Total Dose		= 10^{-7} dpa
(1)	Average concentrations of point defects (at/at)	
	Average concentration of vacancies	= 6.075×10^{-11}
	Average concentration of interstitials	= 8.316×10^{-27}
(2)	Leakage constant of Frenkiel Pairs to different sinks (at/at/sec)	
(2-A)	Leakage constant of vacancies to sinks	
	Leakage constant of vacancies to all sinks	= 60.24
	Leakage constant of vacancies to dislocations	= 23.77
	Leakage constant of vacancies to voids	= 36.48
(2-B)	Leakage constant of interstitials to sinks	
	Leakage constant of interstitials to all sinks	= 1.592×10^{6}
	Leakage constant of interstitials to dislocations	= 6.576×10^{5}
	Leakage constant of interstitials to voids	= 9.345×10^{5}
(3)	Emission rates of vacancies (at/at/sec)	
	Emission rate from vacancy loops	= 4.056×10^{-13}
	Emission rate from interstitial loops	= 7.955×10^{-10}
	Emission rate from voids	= 7.168×10^{-12}
	Emission rate from dislocations	= 2.857×10^{-9}
	Total emission rate of vacancies	= 3.66×10^{-9}
(4)	Rate of recombination of vacancies and interstitials	= 2.509×10^{-25}
(5)	Leakage rate of vacancies to all sinks (at/at/sec)	= 3.66×10^{-9}
(6)	Leakage rate of interstitials to all sinks (at/at/sec)	= 1.324×10^{-20}
(7)	Radii of voids and loops in angstroms	
	Void radius	= 40.
	Interstitial loop radius	= 825.5
(8)	Rate of change of void and loops radii in cm/sec	
	Rate of change of void radius	= -8.511×10^{-14}
	Rate of change of interstitial loop radius	= -2.616×10^{-12}
(9)	Number of vacancy loops and fraction of vacancies retained in them	
	Number of vacancy loops	= 3.112×10^{12}
	Fraction of vacancies in loops	= 4.399×10^{-9}

(10) Changes in initial radii of void and interstitial loop in ang.

Change in loop radius (RIL-RILO) $= -1.156 \times 10^{-3}$

Change in void radius (RV-RVO) $= -9.747 \times 10^{-5}$

V. Concluding Remarks

It has been shown that the steady state theory (SSRT) can be successfully modified to include time dependent effects on a time scale of interest to inertially confined fusion reactors (over at least 10 orders of magnitude in time). The Fully Dynamic Rate Theory (FDRT) formulation can accurately predict steady state electron and heavy ion experimental results on 316 stainless steel and therefore should be invaluable in understanding what effect changes in temperature, displacement rate, dislocation density, effective defect migration energy, etc., have on the ultimate swelling of that alloy. Such parametric studies have now begun and will be the subject of future papers.

Unfortunately, it is not possible to determine how accurately the FDRT predicts swelling in pulsed systems because there is no experimental data to compare with. One might turn this around and look at the optimistic side by observing that the FDRT can now be used to identify interesting regimes for experiments while at the same time determining conditions for which pulsing should have no effects. Future work in this area is absolutely necessary before any large scale reactor systems can be built.

Finally, the reader is again reminded of the fact that the entire approach in this paper is only operative in the regime where nucleation has ceased and where transmutation products such as helium have no further effect on the microstructure. A complete treatment of the problem must include these effects but such an endeavor is by no means trivial.

Acknowledgement

This work was prepared by the University of Wisconsin as an account of work sponsored by the Electric Power Research Institute, Inc. (EPRI), and Wisconsin Electric Utilities Research Foundation (WEURF).

References

[1] S. D. Harkness and C. Y. Li, Proc. of the International Conf. on Rad. Induced Voids in Metals, Albany, New York, (1971), p. 798.

[2] S. D. Harkness and C. Y. Li, Rad. Damage in Reactor Materials, Vol. II, (1969) p. 189, IAEA, Vienna.

[3] S. D. Harkness and C. Y. Li, In Corbett et al., (1971) p. 798.

[4] H. Wiedersich, Rad. Effects, Vol. 12 (1972), p. 111.

[5] A. D. Brailsford and R. Bullough, J. Nucl. Mat. 44 (1972) p. 121.

[6] A. D. Brailsford and R. Bullough, AERE Report, T-P-486 (1972).

[7] R. Bullough, B. L. Eyre and R. C. Perrin, Harwell Report, AERE-R6284 (1969).

[8] R. Bullough and R. C. Perrin, Proc. of the International Conf. on Rad. Induced Voids in Metals, Albany, N. Y. (1971), p. 769.

[9] A. J. E. Forman, AERE Report, R-7135 (1971).

[10] R. Bullough, B. L. Eyre and R. Krishan, Proc. R. Soc. Lond. A. 346, (1975) p. 81.

[11] N. Ghoniem, G. L. Kulcinski, Univ. of Wis. Fusion Design Memo, UWFDM-181 (1976).

[12] C. W. Gear, Numerical Initial Value Problems in Ordinary Differential Equations (Prentice Hall, Englewood Cliffs, N. J., 1971).

[13] M. J. Makin and G. P. Walters, Proc. of Conf. on Physics of Voids (ed. by R. S. Nelson), published as a Harwell Report, AERE R-7934 (1975).

[14] D. J. Mazey, R. S. Nelson and J. A. Hudson, J. Nucl. Mat. 41 (1971), 257.

[15] T. W. Williams, Proc, of B.N.E.S. Conf. on Voids Formed by Irradiation of Reactor Materials (ed. D. F. Pugh, M. H. Loretto and J. H. Harris) (1971).

[16] Y. H. Choi, A. L. Bement and K. C. Russel, Rad. Effects Conf., Gatlinburg, Tenn. (1975).

[17] G. R. Odette and R. Myers, paper submitted for publication to the J. of Nucl. Mat., Oct. 1975.

[18] T. W. Colin and R. W. Balluffi, Phys. Stat., Vol. 25 (1968) p. 163.

[19] K. H. Westmacott, R. E. Smallman and P. S. Dobson, Metals Sci. Journal, Vol. 2 (1968).

[20] L. B. Loeb, The Kinetic Theory of Gases, (Dover Publications, 1961) p. 140.

[21] Kiritani, J. Phys. Soc. Japan, Vol. 4 (1965) p. 148.

[22] A. Kelly and R. B. Nicholson, Prog. Mat. Sci. Vol. 10 (1963) p. 149.

[23] C. A. English, B. L. Eyre, and J. Summers, AERE Report R7960 (1975).

[24] R. W. Conn, S. Abdel-Khalik, G. A. Moses, E. T. Cheng, G. Cooper, J. Howard, G. L. Kulcinski, E. Larsen, E. Lovell, G. Magelssen, I. Sviatoslavsky, W. Wolfer, F. Barenek, S. K. Chang, R. Droll, N. Ghoniem, T. Hunter, M. Ortman, R. Spencer, G. Shuy, M. Ragheb, Univ. of Wis. Fusion Design Memo, UWFDM-190 (1976).

[25] S. A. Dupree et al., Joint Los Alamos Sci. Lab. - Oak Ridge National Lab. Report LA-4557 (ORNL-4662) (1971).